NEW ULTRA-LOW PERMITTIVITY COMPOSITES FOR USE IN CERAMIC PACKAGING OF Ga:As INTEGRATED CIRCUITS

Annual Report
August 1, 1985 to July 31, 1986

ONR Contract No. N00014-84-K-0721

DARPA Order No. 5157

August 11, 1986

MATERIALS RESEARCH LABORATORY
THE PENNSYLVANIA STATE UNIVERSITY
UNIVERSITY PARK, PENNSYLVANIA 16802

SECURITY CLASSIFICATION OF THIS PAGE

AD-A171 705

REPORT DOCUMENTATION PAGE

1a. REPORT SECURITY CLASSIFICATION Unclassified	1b. RESTRICTIVE MARKINGS
2a. SECURITY CLASSIFICATION AUTHORITY	3. DISTRIBUTION/AVAILABILITY OF REPORT Reproduction in whole or in part is permitted for any purpose of the United States Government
2b. DECLASSIFICATION/DOWNGRADING SCHEDULE	
4. PERFORMING ORGANIZATION REPORT NUMBER(S)	5. MONITORING ORGANIZATION REPORT NUMBER(S)
6a. NAME OF PERFORMING ORGANIZATION Materials Research Laboratory The Pennsylvania State Univ. — 6b. OFFICE SYMBOL (If applicable)	7a. NAME OF MONITORING ORGANIZATION
6c. ADDRESS (City, State and ZIP Code) Materials Research Laboratory The Pennsylvania State University University Park, PA 16802	7b. ADDRESS (City, State and ZIP Code)
8a. NAME OF FUNDING/SPONSORING ORGANIZATION Office of Naval Research — 8b. OFFICE SYMBOL (If applicable)	9. PROCUREMENT INSTRUMENT IDENTIFICATION NUMBER
8c. ADDRESS (City, State and ZIP Code) 619 Ballston Tower 800 N. Quincy Street Arlington, VA 22217	10. SOURCE OF FUNDING NOS. PROGRAM ELEMENT NO. / PROJECT NO. / TASK NO. / WORK UNIT NO.
11. TITLE (Include Security Classification) New Ultra-Low Permittivity Composites for Use in	
12. PERSONAL AUTHOR(S) L.E. Cross	
13a. TYPE OF REPORT Annual Report — 13b. TIME COVERED FROM 8/1/85 TO 7/31/86	14. DATE OF REPORT (Yr., Mo., Day) August 11, 1986 — 15. PAGE COUNT
16. SUPPLEMENTARY NOTATION	

17. COSATI CODES			18. SUBJECT TERMS (Continue on reverse if necessary and identify by block number)
FIELD	GROUP	SUB. GR.	

19. ABSTRACT (Continue on reverse if necessary and identify by block number)

This report documents work performed over the second year of a three-year joint program between the Materials Research Laboratory at Penn State University and Interamics in La Jolla, CA, to develop new ultra-low permittivity composite dielectrics for use in the ceramic packaging of Ga:As integrated circuits. The period covered by this report is August 1, 1985, to July 31, 1986, and the work was supported by ONR Contract No. N00014-84-K-0721 under DARPA Order No. 5157.

Topics for study during this year at Penn State have been:

1. Sol-gel processing of SiO_2 films and monoliths.
2. Sputter deposited SiO_2 film structures.
3. Microporous glass structures.
4. Macro-Defect-Free (MDF) cements.

20. DISTRIBUTION/AVAILABILITY OF ABSTRACT UNCLASSIFIED/UNLIMITED ☐ SAME AS RPT. ☒ DTIC USERS ☐	21. ABSTRACT SECURITY CLASSIFICATION Unclassified
22a. NAME OF RESPONSIBLE INDIVIDUAL	22b. TELEPHONE NUMBER (Include Area Code) — 22c. OFFICE SYMBOL

DD FORM 1473, 83 APR — EDITION OF 1 JAN 73 IS OBSOLETE.

SECURITY CLASSIFICATION OF THIS PAGE

Porous SiO_2 films (porosity ~40%) ranging in thickness from 1 μm to 25 μm with k ~ 2.2 and tan δ less than 0.005 have been prepared by sol-gel process. Porous colloidal SiO_2 gels of 1 mm in thickness with k from 1.6 to 2 and tan δ = 0.001 have also been prepared by sol-gel process.

Reactively sputtered SiO_2 films of thickness 5-10 μm exhibit k ~ 3.4 and tan δ = 0.005. A thin dense layer of accuglass and diamond film has been deposited on the porous SiO_2 film to close the surface porosity and aid in metallization.

For etched porous vycor glass structures, permittivities in the range of 2.5 to 3.0 have been measured with excellent low loss properties. In the microporous vycor evaporated electrode patterns have been used, and the low loss is preserved into the microwave region.

Eight different kinds of calcium aluminate and several silicate cements have been prepared by MDF process and the dielectric properties characterized at low frequency. Calcium aluminate cement loaded with silica microballoons and prepared by MDF process has a k of 4.7.

In a parallel program at Interamics, new families of borosilicate bonded alumina ceramic are being developed. Tapes using both lead and calcium borosilicate glasses have been fabricated and densified at firing temperature at approximately 900°C. Silver has been selected for the preliminary studies of metallization. Test packages using both types of glass bonded ceramics have been fabricated. The dielectric permittivity of lead and calcium borosilicate bonded alumina are 7.5 and 7.9, respectively.

TABLE OF CONTENTS

1.0 INTRODUCTION

This report documents work performed over the second year of a three-year joint program between the Materials Research Laboratory at Penn State University and Interamics in La Jolla, CA, to develop new ultra-low permittivity composite dielectrics for use in the ceramic packaging of Ga:As integrated circuits. The period covered by this report is August 1, 1985, to July 31, 1986, and the work was supported by ONR Contract NO. N00014-84-K-0721 under DARPA Order No. 5157.

Topics for study during this year at Penn State have been:

1. Sol-gel processing of SiO_2 films and monoliths.
2. Sputter deposited SiO_2 film structures.
3. Microporous glass structures.
4. Macro-Defect-Free (MDF) cements.

At Interamics, the objective has been to replace the current high firing temperature (1650°C) alumina dielectrics with lower firing temperature (approximately 900°C) alumina/glass composites. In this approach, both calcium and lead borosilicate bonded alumina are being studied where it is evident that processing temperatures can be reduced to 900°C. Metallization of these composites are being investigated with conductive metals such as gold, silver and copper which are compatible for firing at the lower temperatures with air or nitrogen atmospheres.

In the Penn State program, the sub-tasks are each supervised by a faculty member who is a recognized authority in the materials area under study. The overall program is coordinated by Professor L.E. Cross with the help of Dr. T.R. Gururaja, electrical measurements for all participants are being carried forward on the automated measuring facility under the direction of Paul Moses. Microwave measurements rely mostly upon an HP 8510T measuring system under the direction of M. Lanagan and Dr. Jin-Hun Kim, assisted by Dr. Sei-Joo Jang.

2.0 RATIONALE FOR THE PRESENT APPROACHES

To accomplish the strip line structures at the spacing and wiring densities which will be required for the interconnect systems of high speed Ga:As ICs, studies by B. Gilbert, et al., at Mayo Clinic, indicate that for dimensions which appear feasible in proposed structures, a basic requirement for the supporting insulator will be an exceedingly low dielectric permittivity. The absolute upper limit which can be tolerated is of order $3\varepsilon_o$ and even lower values would be very highly desirable.

Evaluation of possible inorganic dielectrics indicates a lower limit for single phase materials of order 3.85 ε_o in silica glass, thus it is not possible with existing single phase inorganic dielectrics to achieve this very basic requirement of ultra-low permittivity, and a composite approach involving at least one much lower permittivity phase will be essential.

In the approaches taken on this contract, that second phase has been chosen to be gas or vacuum with permittivity 1 ε_o. The focus is then to develop tractable low permittivity inorganic host dielectrics into which a controlled closed pore structure can be introduced by suitable processing. Since any pore structure will necessarily introduce many undesirable "side effects," lower thermal conductivity, reducing mechanical strength, etc., it is most desirable to control the pore network so as to limit it to regions under the strip line traces, where the consequent permittivity reduction is essential.

Although a viable substrate for packaging VLSIs has many other important parameters such as mechanical strength, thermal conductivity, etc., which should be considered, the primary goal in this contract is to develop ultra-low permittivity dielectrics. In this regard, several processing techniques have been explored to prepare ceramic/void nanocomposites with ultra-low permittivity.

3.0 DIELECTRIC MIXING RULES

The basic approach which has been used for lowering k is that of "mixing" with dielectric ceramic pores of controlled geometry which contain air or inert gas with k close to unity. A general question which must be addressed here is the mode of interconnection between the two phases and its effect on the dielectric properties. Since the introduction of pores is associated with a sacrifice in mechanical strength, it is preferred to use a mode of mixing which would keep the volume of the void space as small as possible consistent with achieving the needed level of permittivity.

A listing of four simple dielectric mixing rules are presented in Table I, in which the effective permittivity of the composite is represented as a function of volume fraction of relative permittivities of the two phases[1]. A graphical representation of these mixing rules using SiO_2 glasses and air with k of 3.8 and 1, respectively, is given in Figure 1.

Table I. Dielectric Mixing Rules for Two Phase Composites[1].

$\frac{1}{\bar{K}} = \frac{V_1}{K_1} + \frac{V_2}{K_2}$	$\bar{K} = K_1V_1 + K_2V_2$
a) Series Mixing	b) Parallel Mixing
$\ell n\bar{K} = V_1\ell nK_1 + V_2\ell nK_2$	$\bar{K} = \frac{V_2K_2(\frac{2}{3} + \frac{K_1}{3K_2}) + V_1K_1}{V_2(\frac{2}{3} + \frac{K_1}{3K_2}) + V_1}$
c) Lichtenecker's Logarithmic Mixing	d) Maxwell's Mixing

$\bar{K}$ = average relative dielectric permittivity.
K_1, V_1 = relative dielectric permittivity and volume fraction of phase one.
K_2, V_2 = relative dielectric permittivity and volume fraction of phase two.

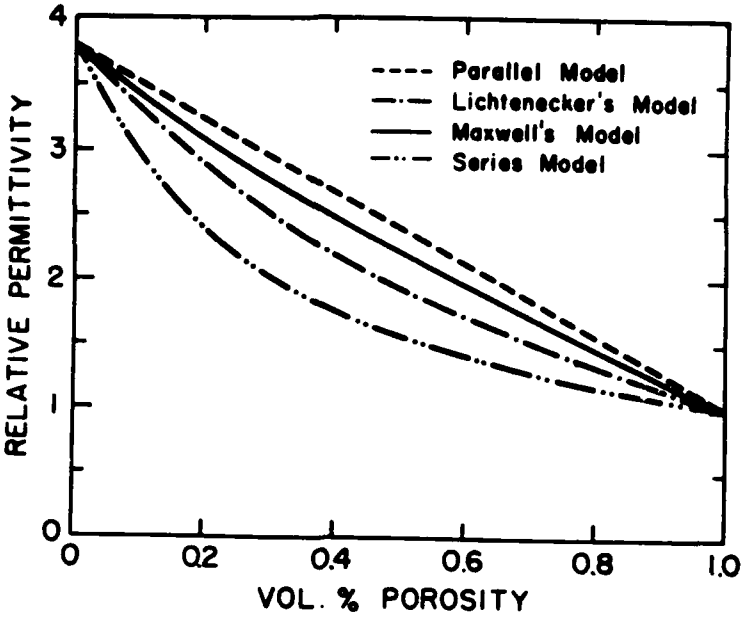

Figure 1. Relative permittivity of porous silica glass as a function of volume percent porosity for series, parallel, Maxwell's and Lichtenecker's mixing rules.

In parallel mixing, the dielectric is in the form of a room and pillar structure with columns of dielectric dominantly parallel to the electric field. In series mixing, layers of the two phases are stacked alternately with E-field normal to the layers. The series mode is clearly more advantageous in reducing the permittivity but obviously difficult to realize in practical structure. For a composite dielectric in which neither parallel nor series mixing is strongly preferred, i.e. systems with random connectivity, the empirical Lichtenecker's logarithmic mixing rule is often applied (Table I, Figure 1). In the case where small spherical pores are uniformly distributed in the matrix phase, Maxwell's mixing rule is applicable.

It should be noted in all the above calculations, an assumption is made that the composite feature is small compared to the wavelength. Even for 10 GHz frequency components, the wavelength is of the order 1.5 cm in a material with k of 4. Clearly this dimension is very much larger than the scale of any of pore structure envisaged, so these simple calculations provide an initial

guide for selecting pore volumes which will be required for any given host permittivity and architecture.

4.0 SOL-GEL PROCESSING OF SiO_2 STRUCTURES

The objective of the sol-gel processing SiO_2 is two fold. 1) To develop a method to spin cast 1 to 25 micron thick films of porous SiO_2. 2) To explore the possibility of forming colloidal SiO_2 gels which are thick enough to support multilevel wiring. These studies are under the direction of Dr. R. Roy and involve the work of two graduate students, U. Mohideen and W. Yarbrough.

4.1 Thick Film Coatings of Porous SiO_2

Flow chart for processing of sol-gel derived SiO_2 thick films is presented in Figure 2. A commercial Ludox AS-40 sol (DuPont, Wilmington, DE) was mixed with 3 weight percent PVA solution in water. The viscosity of the solution was allowed to increase through the evaporation of water. When the viscosity reached 10-100 poise, the solution was applied on a low resistivity (0.001-0.006 ohm-cm) silicon substrate (Pensilco Corp., Bradford, PA) and spun at 2000-3000 rpm for 5 minutes. The film was dried in open air for 12h to allow shrinkage through evaporation of water and then dried at 100°C to get rid of residual water present. The polymer network provides the mechanical strength to the colloidal gel during the drying process thereby overcoming the cracking behavior. The film was heated at the rate of 2°C/min to 500°C and held there for about 1h. Even temperatures as low as 350°C could be used for firing if a continuous flow of oxygen is used in the furnace. The thickness of the films ranged from 1 to 25 microns depending on the viscosity of the solution. The thickness of the films were measured using both a profilometer and a scanning electron microscope.

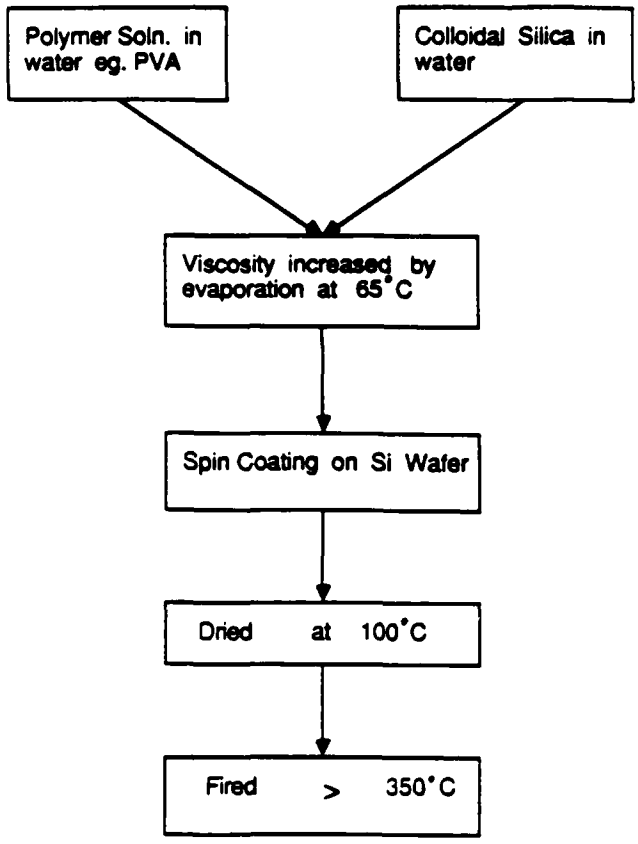

Figure 2. Flow chart of processing of sol-gel derived SiO_2 films (thickness = 1-25 μm).

Samples were prepared for permittivity measurements by sputter coating a 1 inch diameter gold electrode on the SiO_2 film. The back surface of the low resistivity silicon wafer served as the other electrode. Low frequency (100 Hz to 100 kHz) capacitance and loss tangent of SiO_2 films were measured using HP multifrequency LCR meters (Models 427A-A, 4275-A) in the temperature range of -50 to 100°C. The relative permittivity and loss tangent of a representative sample are plotted in Figure 3. The relative permittivity was approximately 2.2 with loss tangent below 0.005 up to 100°C. The dissipation factor was found to be below 0.03 even after exposing SiO_2 films to humid atmospheres for over two weeks.

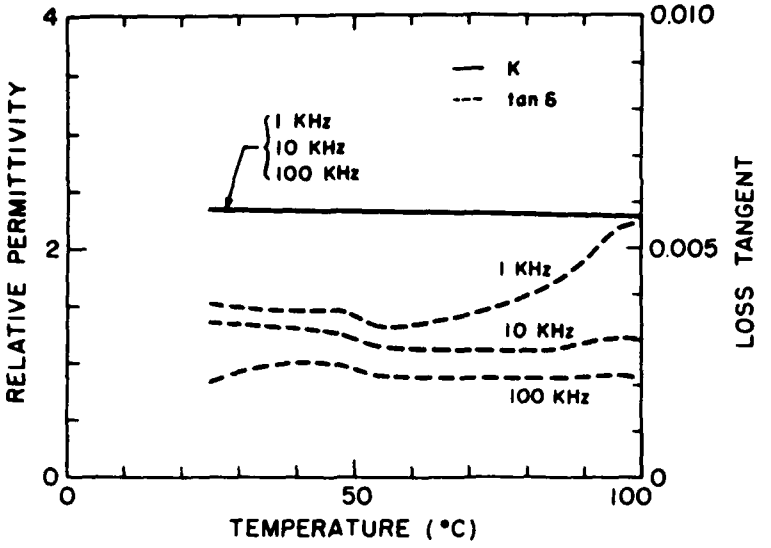

Figure 3. Relative permittivity and loss tangent as a function of temperature of sol-gel derived SiO_2 films.

At wavelength scanning ellipsometer (Sopra, Bois-Columbus, France) was used to determine the porosity in SiO_2 films and it was found to be approximately 40%. From Figure 1 it can be seen that the estimation of effective permittivity using Lichtenecker's random mixing model with 40% porosity agrees well with the measured k of 2.2.

Thus, this process gave both the required thickness and also the appropriate dielectric properties specified for packaging Ga:As ICs. Dielectric measurements on these films in the GHz frequency range are being performed. It should be mentioned here that the ability to process the films at 350°C is an added advantage of this technique.

Sol-gel processed SiO_2 films of 1-2 microns in thickness developed at Penn State are being evaluated by Dr. Dan Younger at Honeywell, Solid State Electronics Devices Section. The low frequency dielectric properties reported from Honeywell on these materials are in excellent agreement with our measurements. The ultra-low permittivity SiO_2 films are intended for use by Honeywell as an interlayer dielectric on multilayer metal integrated circuit fabrication process. The results from an initial study are very promising.

The main concern at this point is the presence of 0.08% sodium in the Ludox sol which are highly detrimental to the semiconductor devices. Attempts are being pursued to prepare sodium-free SiO_2 colloids.

4.2 Colloidal SiO_2 Gels

In this method, Cab-O-Sil L90, a relatively low surface area (~90 m^2/g) fumed silica containing <2 ppm Na_2O (Cabot Corp., Tuscola, IL) was used to prepare a colloidal sol in water. This could be readily prepared by dispersing in high shear rates at solid levels of ~20 weight% using either acidic or basic stabilization, i.e., at pH levels of ~3 or 9-11. The acidic sol was metastable as prepared and formed a weak gel at long standing (2-3 months) at room temperature. The basic sol was stable indefinitely.

Xerogels were prepared from such sols by two different methods. In the simplest case, a xerogel was obtained by slowly evaporating the liquid. Samples suitable for dielectric measurements could not be obtained this way as significant amounts of warpage and fracture usually result from the large tensile stresses developed at the surface during drying. An alternative method was to form stiff gel by adjusting the pH to near neutral. This gel is then pressed into a pellet using porous media (e.g. graphite) above and below in a 2.54 cm I.D. steel pellet press. Most of the free fluid volume is removed in this step, which results in a gel body of sufficient integrity to resist further shrinkage on drying.

The resulting gel pellets were dried in air at room temperature for 16-24h and then fired to temperatures varying from 900°C to 1200°C for periods varying from 2 to 12 h. Firing at 900°C for 1h in air was sufficient to produce a very lightly sintered xerogels of 55 to 65 volume% porosity. There is little or no shrinkage of the body below 1000°C. These firing conditions

(900°C for 12h) produced a body of sufficient mechanical integrity to permit polishing and application of electrode.

Pellets of thickness close to 1 mm were prepared for dielectric measurements by sputter coating gold electrodes on either side. The measurements were performed as described earlier, and the results on three samples are presented in Table II. The relative permittivity of porous colloidal SiO_2 gels were found to be in the range of 1.6 to 2.0. The Lichtenecker's random mixing rule, using the estimated pore volume in the gel, gives an excellent agreement to the data. The dielectric loss tangent in the samples was found to be extremely low in the range of 0.001.

Table II. Relative Permittivity of Porous Colloidal SiO_2 Gels Fired at 900°C for 12h.

Sample No.	1	2	3
Vol%	58.5	64.9	63.7
Measured K' (10 MHz)	2.07	1.94	1.87
Loss Tangent	0.0009	0.0007	0.0009
Correction for Stray Cap. ASTM D150-81	-0.29	-0.31	-0.29
Corrected K'	1.78	1.63	1.58
Predicted K' (Lichteneckers Rule)	1.74	1.60	1.62
Parallel Mixing	2.15	1.98	2.01
Series Mixing	1.44	1.34	1.36

The pore structure of the xerogel remains open and interconnected in materials calcined at temperatures below ~110°C. This means that additional materials can be readily diffused into the open pore network, including

radiation curable resins for the development of vias and conductor channels. In spite of the high and accessible porosity of such bodies, it has not been found necessary to take any special precaution to protect surfaces from atmospheric moisture or other contaminants. This is believed to be due to the high purity of the silica used, and the removal of chemisorbed water at temperatures ~W900°C to form a relatively hydropholic surface.

5.0 SPUTTER DEPOSITED SiO_2 FILMS

This study was under the supervision of Dr. R. Messier and was carried forward by A. Das. In this study, RF sputtering technique was used to generate porous SiO_2 films. Since the deposition rate using SiO_2 as the target material is known to be very slow (approximately 0.12 micron/h), it becomes impractical to generate 25 micron thick films using this method. Two alternate approaches have been investigated.

In the first approach, uniform 25 micron thick amorphous Si films were first deposited. The morphology of these films were columnar, with the column diameter varying from 0.1 to 0.3 microns. This columnar structure was then anisotropically etched using the faster etch rates of the low density regions between the columns as compared to the columns themselves. Two etching techniques, one wet (chemical) and the other dry (reactive ion etch), were attempted. The etched films were thermally oxidized in dry O_2 at 1100°C. Etching out the regions around the columns would enable the oxidation to proceed laterally into the columns rather than down the columns. Etching step was also used to introduce porosity into the films.

A limitation of this approach was encountered during the thermal oxidation due to the tremendous volume expansion as the Si-Si bonds are broken and Si-O bonds are formed. This led to severe cracking in the films. Because

of this difficulty, an alternate route was investigated to prepare porous SiO_2 films.

For reactive sputtering, a 5" Si (99.99% purity) was used as the target in the RF sputtering unit (MRC model SCS8632). Three different gas pressures were selected: (a) P_{AR} = 27 mtorr and P_{02} = 3 mtorr (10%), (b) P_{AR} = 37 mtorr and P_{02} = 3 mtorr (7.5%), (c) P_{AR} = 44 mtorr and P_{02} = 1 mtorr (2.2%). The RF power was maintained at 120 watts and the substrate target distance was 3.5 cm in all the cases. The films were deposited on 2.54 cm diameter low resistivity (0.001-0.0006 ohm-cm) p-type Si wafers.

The dielectric measurements were performed on the films as explained earlier. Figure 4 shows the relative permittivity as a function of temperature for the three deposition conditions. As the total pressure in the system is increased, more porosity is introduced and the permittivity is reduced. High pressure are being investigated which should decrease the permittivity further to the desired value of 3. The loss tangent were found to be less than 0.005 in all the films.

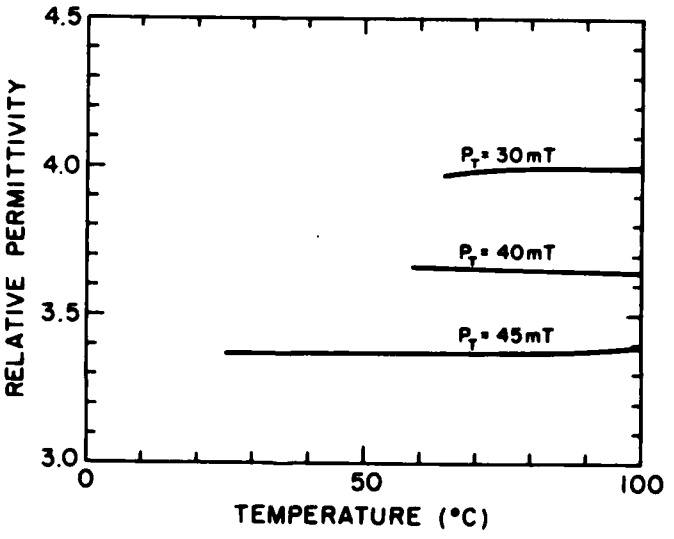

Figure 4. Relative permittivity vs. temperature of reactively sputtered SiO_2 films (P_T is total gas pressure in mtorr).

5.1 Effect of Surface Roughness on Sputtered Films

The surface roughness is known to effect the morphology and density of sputtered films. To study this phenomenon, reactively sputtered SiO_2 was deposited on single crystal Si wafer and on fine grained alumina coated with gold, under the same sputtering conditions. SEM micrographs (Fig. 5a and b) compare the surface morphology of the films. The film on the alumina substrate is much coarser as compared to that on Si wafer.

5.2 Accuglass and Diamond Coatings on Porous Films

To prevent problems of electroding rough surfaces and also to prevent moisture penetration, spin-on-glass (SOG) was used to coat the surface of sputtered films with a thin film of SiO_2. The spin-on-glass used was Accuglass 203 (Allied Corporation). It is a solution of silicon-oxygen polymeric material in an alcohol/ketone solvent. This commercially available material is primarily used for planarization of metallization surfaces in the microelectronic industry. SOG has a relative permittivity of 8 when cured at 400°C, and 4.2 when cured at 800°C.

The capping films was spun on at 2000 rpm, for 20 seconds. Figure 6a and b compare the surface of a reactively sputtered film before and after accuglass coating.

Thin diamond films are also being deposited on reactively sputtered porous SiO_2 to increase the scratch resistance and mechanical strength of the film. The relative permittivity of diamond being approximately 5.5 is not expected to increase substantially the relative permittivity of the composite structure.

The procedure for coating thin films of diamond has been developed at the Materials Research Laboratory. The films are prepared by reacting methane and hydrogen gases in a microwave plasma. In this study, approximately 500A°

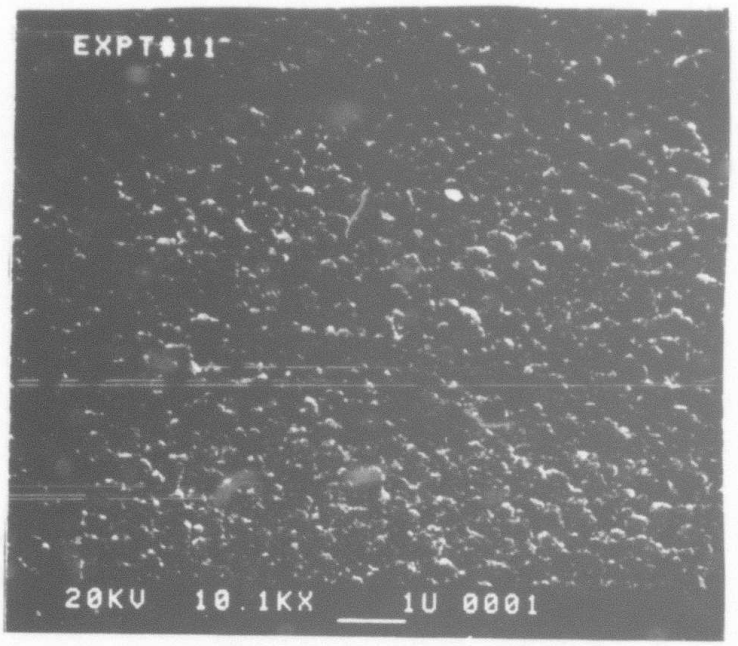

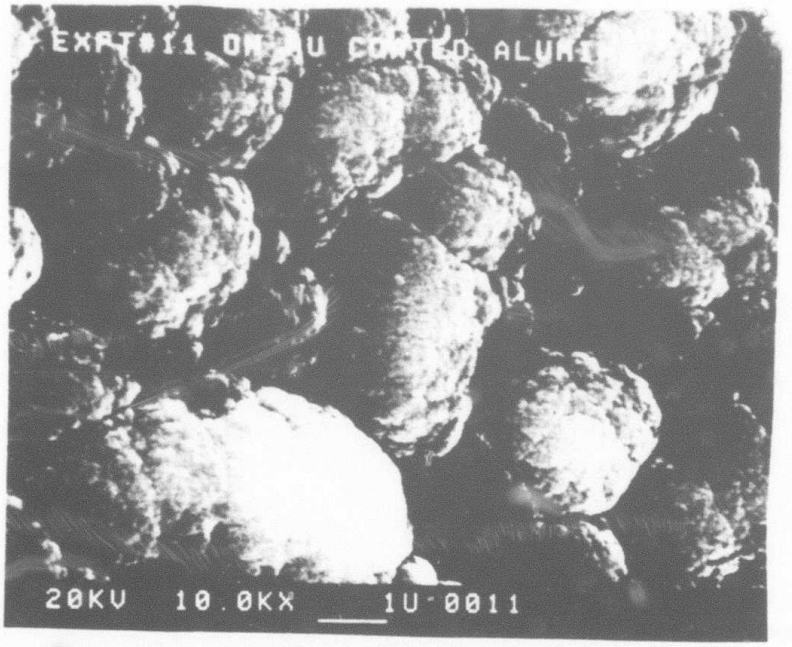

Figure 5. SEM micrograph of surface morphology of reactively sputtered SiO_2 films (a) on Si wafer, and (b) on fine grain alumina substrate.

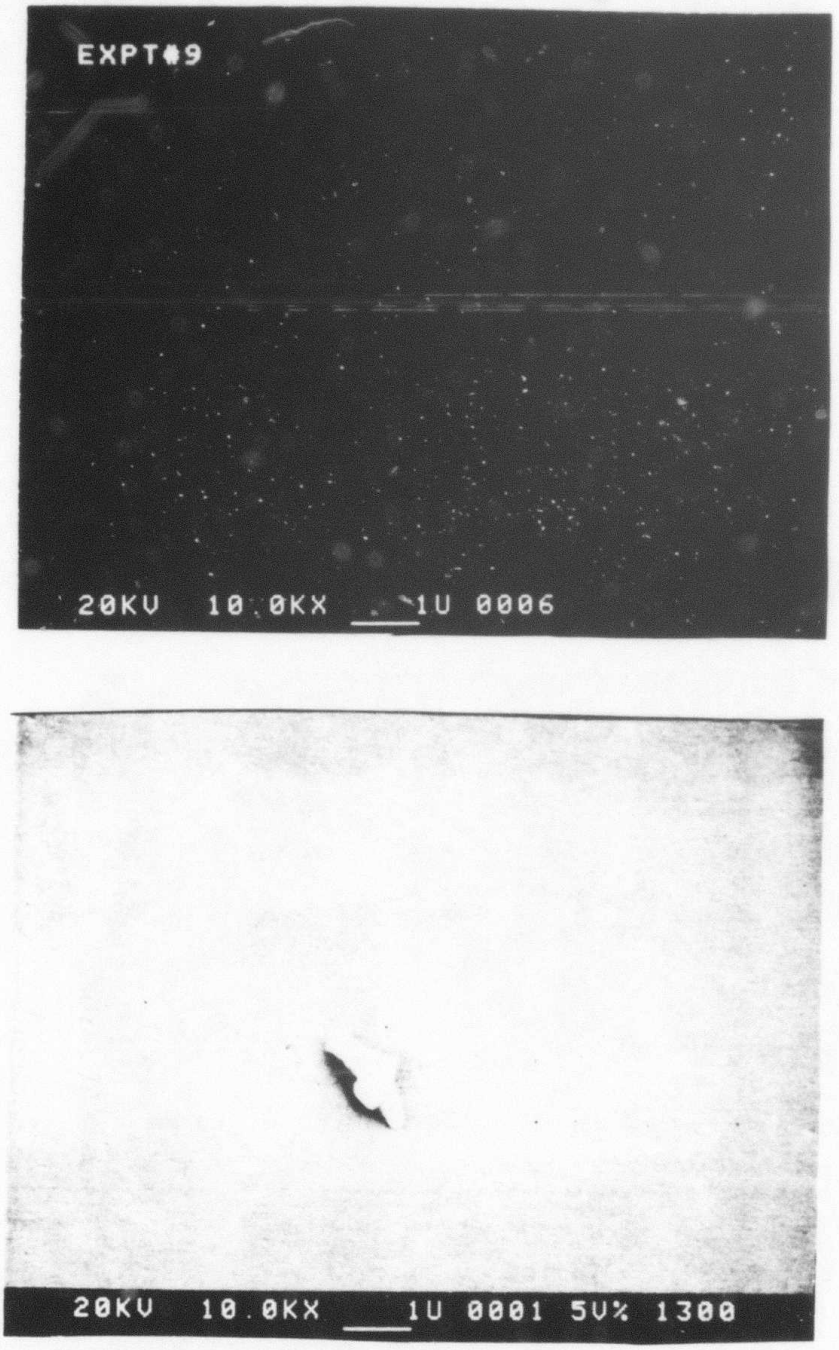

Figure 6. Surface of reactively sputtered SiO_2 film (a) before accuglass coating and (b) after accuglass coating.

thick layer of diamond was deposited on reactively sputtered SiO_2 film. The relative permittivity of the composite structure was found to be 3.6.

5.3 Future Work

As a part of future work, we would be measuring the thermal expansion coefficient, thermal conductivity of these films. The other study would be in the area of moisture penetration into porous films. Various reactively sputtered films will be subject to different conditions of temperature and humidity and their moisture content as a function of depth will be obtained using the secondary ion mass spectrometry (SIMS).

6.0 MICROPOROUS GLASS STRUCTURES

Work in this area is supervised by Dr. R.E. Newnham and is carried through by J. Yamamoto. The focus in this study was to take commercially available Corning 7930 porous vycor glass and to investigate the dielectric properties in the microwave region of both as-received and leached porous structures. The average pore diameter in this material is approximately 40A° so that electroding by sputtering or evaporation is not a problem.

Measurements of permittivity and loss tangent over the frequency range from 4 kHz to 10 MHz at temperatures from 25 to 125°C show excellent low permittivity (3.5) and loss tangent (0.005). To lower the permittivity a little further, a post leaching with 2 and 10% HF was tried for times of one and five minutes. After leaching, the porous vycor samples were soaked in boiling HCl to eliminate any impurities, cleaned in deionized water, and heat treated at 300 to 700 for 4 hrs in flowing oxygen. Dielectric measurements at 2.5 GHz were performed on HF treated and untreated porous vycor glass using resonance perturbation technique in a re-entrant cavity. The technique is based on measuring the change in the impedance of the cavity with the

introduction of the sample. A block diagram of the equipment is shown in Figure 7.

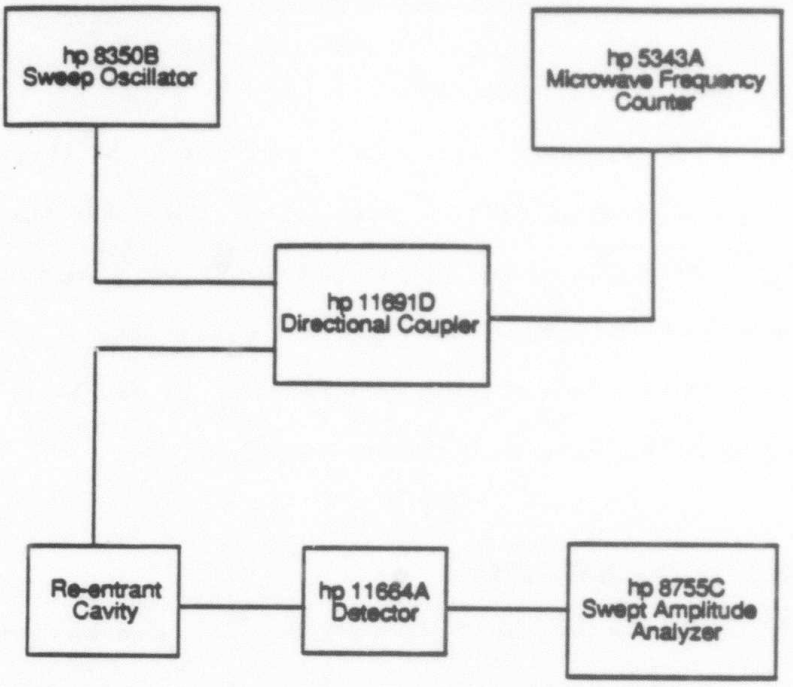

Figure 7. Schematic diagram of microwave dielectric measurement set up.

Figure 8 shows the effect of leaching and heat treatment on dielectric permittivity. From the figure, it can be observed that k of unleached microporous silica was reduced with increasing soak temperatures reaching a minimum of 2.6 at 700°C, with loss tangent below 0.001. The heat treatment was shown to be effective in removing moisture and impurities absorbed in the glass. The relative permittivity of the 2% HF leached sample was lower than the untreated glass over the entire temperature range. The 10% HF leaching did not show any reduction in the permittivity over the untreated glass, which may be attributed to the collapse of the silica structures.

The microwave dielectric measurements on porous vycor have been extended to higher frequencies in the GHz range using transverse magnetic (TM) cavity method which is more reliable and accurate. Two cavities were used to make measurements at 3 and 6 GHz. The relative permittivities of porous vycor

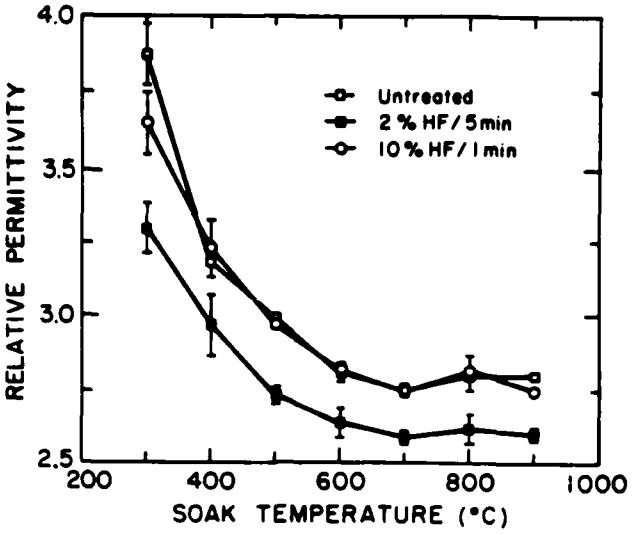

Figure 8. Effect of leaching and heat treatment on relative permittivity of porous vycor glass.

measured by this technique were similar to the results from the re-entrant cavity technique.

Currently, water adsorption studies on porous vycor are being conducted, the results of which will be reported in the next quarter.

7.0 MACRO-DEFECT-FREE CEMENTS

This area of study is the responsibility of Dr. D.M. Roy and Dr. B.E. Scheetz with graduate assistants Paul Sliva and Pamela Kistler. Rationale for initiating studies in this area of chemically bonded ceramics for substrate applications are (i) In the chemical consolidation process of cement curing, there is a change of phase to a hydrated form which is of lower density than the parent powder. Thus it is in principle possible to obtain full mechanical integrity without shrinkage. Since for most ceramic systems, it is the reproducibility and control of shrinkage which limits wiring resolution and density. Zero shrinkage could be most valuable. (ii) The very low temperature curing of cement permits a wide range of techniques for introducing a second phase such as hollow glass microspheres or a fugitive phase which can be lost in subsequent processing to produce the controlled pore structures which are necessary for permittivity control. The low

temperature processing also permits the use of high conductive metals for interconnects.

However, a major disadvantage of cement is their inherent large porosity. Bulk mechanical properties can be related to porosity and thus it is a key factor in controlling the ultimate strength of a cement. One approach to increasing the mechanical strength of a cement is based on eliminating all but the fine porosity (<10 μ) to produce macro-defect-free (MDF) cement. The recent work of Birchall and co-workers indicates that cement produced by MDF processing has superior mechanical properties over conventionally processed cement[2-3]. Larger pores can be eliminated by reducing the water:cement (w/c) ratio ($\leq$0.20) and through the use of conventional ceramic processing (shear mixing, extrusion, die pressing, calendering).

The work on MDF processing cements and evaluation of their dielectric and mechanical properties have been performed on calcium aluminate and silicate based cements. For each of the classes of cements, it is necessary to go through

1. Characterization of the precursor cements.

2. Investigation of possible methods to produce macro-defect-free character and their influence on dielectric properties.

3. Determination of the effect of additives, particularly silica micro-balloons to reduce the observed permittivity levels.

In the subsequent sections, the results of our work on calcium aluminate will be described in detail and salient features on the silicate based cement will be presented.

7.1 Calcium Aluminate Cements

In the first part of the investigation, commercially available calcium aluminate cements were processed by the MDF method to evaluate their

dielectric properties for substrate applications. Later one type of cement was loaded up to 70 volume% with hollow glass microspheres to study the effect of controlled pore structure on permittivity. A brief report of the study is presented here. Further details are included in Appendix C and D.

7.1.1 MDF Processing

Several types of commercial calcium aluminate cements supplied by Lone Star Lafarge, Inc. (Norfolk, VA) and ALCOA (Pittsburgh, PA) were investigated. The Lone Star Cements are classified as a SECAR^{TM} cement followed by a number depicting the weight percent Al_2O_3 content. All the ALCOA cements had approximately 80 weight percent of Al_2O_3. Samples were prepared by hand mixing 50 gm of cement in 11.11 gm of 11 wt% PVA solution resulting in a water to cement ratio of 0.20 and a PVA/(water and cement) of 0.018. The dough was then homogenized and trapped air removed by high shear mixing under vacuum in C.W. Brabender preparation mill (Hackensack, NJ). The resulting dough was prepared into 2.54 cm diameter discs in a steel die coated with teflon mold release at a pressure of 138 MPa for 10-15 seconds. Cement discs were cured at room temperature in a dessicator.

7.1.2 Low Frequency Dielectric Response

Dielectric permittivity and loss tangent measurements were performed as explained earlier with sputter coated gold electrode on either side of the discs. Typical low frequency dielectric response for calcium aluminate cement is given in Figure 9. The permittivities are quite low considering that the samples contain both unbound water and PVA. The SECAR cements show a wide range of permittivities. Permittivities for the SECAR 80 series cements are high because of their high alumina content. SECAR 71 and SECAR 60, as seen in Figure 9, have lower permittivity in the range of 4 to 6 and relatively flat

frequency dependence. The dielectric permittivity of ALCOA cement with approximately 80 wt% Al_2O_3 was ~8, with a frequency response similar to that of SECAR 80 fast set (Fig. 9). Dielectric loss tangent in both SECAR and ALCOA cement samples were about 0.10 at 100 Hz decreasing to 0.02 at 1 MHz. In these cements cured under ambient conditions, the dominant transport of charge is the unbound water-PVA network, which is probably responsible for the large frequency dependence of k and loss tangent up to 10 kHz.

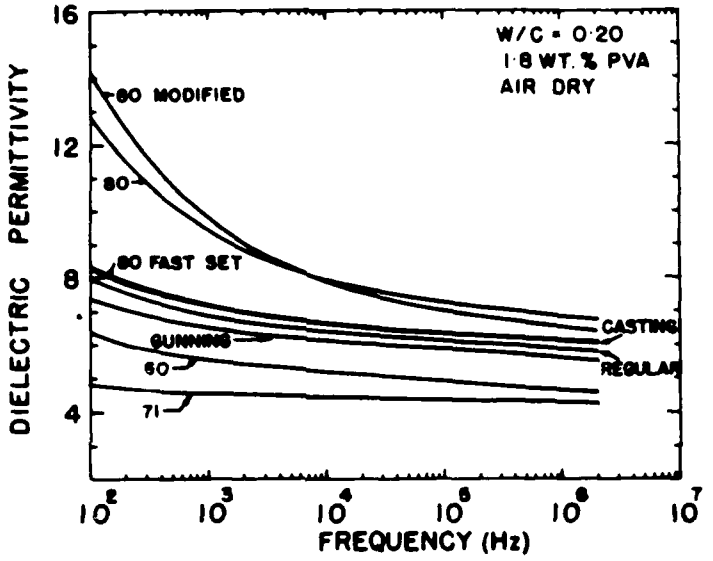

Figure 9. Relative dielectric permittivity of calcium aluminate cements containing 1.8 wt% PVA, a water-cement ratio of 0.20, cured in air as a function of frequency.

7.1.3 Effect of Microballoon Loading on Permittivity

From the above study, it is clear that the MDF processed calcium aluminate cement cannot attain the ultra-low permittivity required for packaging high speed Ga:As ICs. Therefore, introduction of closed porosity via hollow glass microspheres was considered to lower the relative permittivity of calcium aluminate cement. Although samples prepared using SECAR 60 and 71 possessed the flatest frequency response of dielectric permittivity (between 4 and 6) and therefore have the highest potential for

use as dielectric substrate, SECAR 80 was chosen for this study. SECAR 80 exhibits the highest dielectric permittivity of all the cements ranging from ~13 at 100 Hz to ~7 at 1 MHz. Consequently, it is anticipated that subtle differences in the dielectric permittivity upon the addition of glass microspheres may be more pronounced in SECAR 80 as compared with SECAR 60 to 71.

High strength microballoon spheres FTD-202 (Emerson and Cuming) with an average particle diameter of 65 microns and a wall thickness of 1 to 2 microns were used in the study. Cement samples were prepared as explained earlier with microsphere loadings of 0, 27.5, 40, 50, 60 and 70 volume percent. Because of the high shear mixing, a large fraction of microballoons were destroyed during processing. Effective loadings of microspheres was estimated by comparing the experimental density with the theoretically calculated densities. Microsphere loadings of 27.5, 40, 50, 60 and 70 percent were found to correspond to effective loadings of 10.6, 21.7, 10.6, 14.1 and 19.7.

The dielectric mixing rules for cement-microsphere composite, assuming relative permittivities of 6.8 and 1.17 taken at 1 MHz for the cement and glass microspheres, are graphically represented in Figure 8. Using the relative permittivity of each composite at 1 MHz and its known effective porosity, the data for five cement-microsphere composites are plotted in Figure 10. As seen in the figure, Maxwell's as well as Lichtenecker's models are closest to the experimental data. The loss tangent for all the composites was approximatley 0.02 at 1 MHz.

Thus microsphere loadings in SECAR 80 cement resulted in up to 30% lower permittivity. Application of this approach of introducing a closed pure structure into the cement could obviously be further enhanced by using a stronger microsphere or providing softer processing. Additionally, although

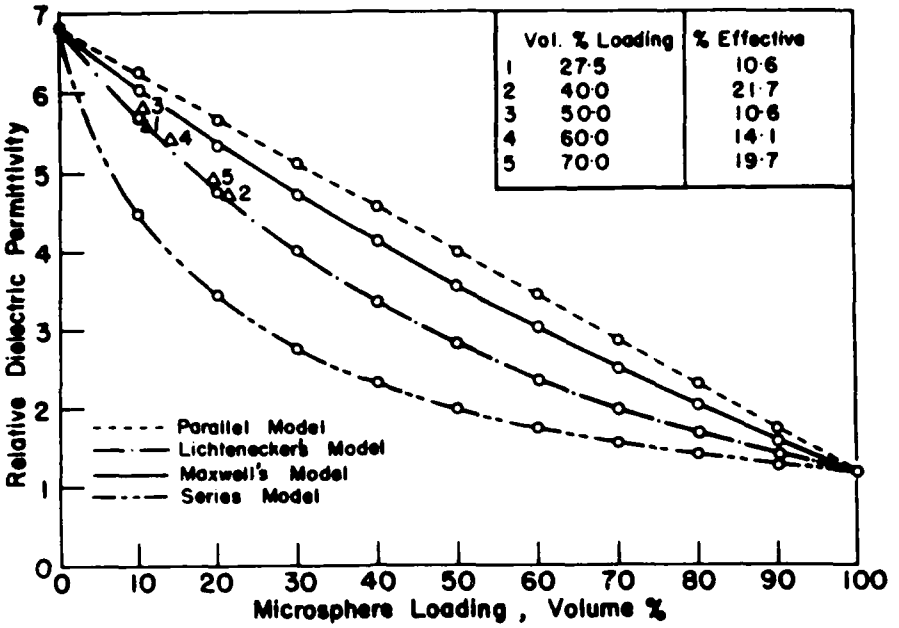

Figure 10. Relative dielectric permittivity of cement-microsphere composites as a function of volume percent microsphere loading for series, parallel, Maxwell's and Lichtenecker's mixing rules.

SECAR 80 was used in this study for demonstration purposes, SECAR 60 to 71 would provide a much better baseline matrix material for further reduction of the dielectric permittivity. For example, the relative dielectric permittivity of 4.3 for SECAR 71 (at 1 MHz) would require the addition of only 30 volume percent microspheres to lower the dielectric permittivity of the composite to 2.9.

7.1.4 Future Work

The primary investigation at present is to determine the exact role of the plasticizer in controlling cement paste rheology and in the final binding of the cementitious phases. It is suspected, in the case of polyvinyl alcohol (PVA) and a few other water soluble plasticizers, that calcium from the cement reacts with the plasticizer to form a cross-linking network that aids in the cohesion of the cement particles. Inorganic plasticizers such as ammonium polyphosphate are a possible substitute as a rheological aid. Investigations will include rheological behavior, reaction with the cement and the effect of thermal treatment on strength, shrinkage and dielectric properties.

The feasibility of tape casting calcium aluminate cement into thin substrates is also under investigation. The approach is to plasticizer the cement, tape cast and sinter the green body after metallization as in conventional multilayer processing. The advantage over conventional glass bonded ceramic will be in the much lower firing temperatures and lower shrinkage associated with the chemical consolidation of the cement material.

7.2 Silicate Based Cements

This area of study focuses on the modification and processing of a silicate-based cement to obtain higher mechanical strength without degradation of the dielectric response. The cement was modified by the addition of one or more of the following materials:

(1) A water-reducing agent, specifically a sulfonated naphthelene derivative used to improve the workability of the cement.

(2) A water-soluble polymer, specifically a cellulose derivative required to increase the plasticity of the cement.

(3) A calcium-magnesium-aluminum-silicate glass and a fine-particulate silicate used to vary the particle size distribution of the cement to obtain higher density packing.

(4) Hollow silica microspheres used to control the void volume in the material.

The processing techniques used in this study included:

(1) Extrusion and calandering of high polymer content materials.

(2) Room-temperature uniaxial and warm isostatic pressing of low-polymer content materials.

(3) Vibro-compaction and calandering of cements containing microspheres.

(4) Heat treatment of the polymer-containing materials.

Results of the experiments on cements containing a cellulose derivative have shown that materials with higher polymer contents required longer curing times to develop strength and were more porous than lower polymer-content materials. Also, the materials which were heat treated to remove the polymer were more porous, less dense, weaker, and have lower permittivities than the corresponding unfired materials. Increasing the firing temperature tends to decrease the strength and density, and increase the porosity of the material.

The effects of the various densification techniques on the properties of the modified cements have also been compared. Calandered materials are weaker, less dense, more porous, and have lower dielectric constants than with uniaxially or isostatically pressed materials. In addition, extruded materials are less porous than their calandered counterparts. However, isostatic pressing of the as-extruded material yields a more dense material. Pressing or calandering of the extruded material to form larger pieces yields more porous, weaker materials than directly calandered or pressed materials due to macropores remaining between layers of the as-extruded material. Isostatically pressed materials are more porous and have a slightly lower dielectric constant than uniaxially pressed materials. However, the two materials are similar in strength.

Modification of the cement with various particle size silicates does not improve the properties of the cement. The porosity of the material is decreased, but there is no significant improvement in the strength of the material. In addition, the dielectric constant is increased significantly.

Pressing of cements containing the hollow microspheres tends to crush these spheres. Less vigorous processing techniques, such as vibro-compaction and calandering, seem to leave the spheres intact. The vibro-compacted materials were found to be stronger, more dense and less porous then their calandered counterparts.

For some representative properties, consider the comparison of uniaxially and isostatically pressed materials. The material was a mixture of a silicate-based, white cement (Type I) and the water-soluble polymer, carboxymethyl hydroxy ethyl cellulose. The water-to-cement ratio was 0.05 and polymer-to-cement ratio was 0.01. The paste was pressed into disks at approximately 10,000 psi. Subsequently, half the disks were cured over water at 90°C and the remaining disks were isostatically pressed at 2000 psi and 90°C for 24 hours. Sample disks were then fired to 450°C and 700°C at 5°C/min and held at temperture for 5 hours. The splitting strength, density, and porosity of the unfired material along with the materials fired to 450°C and 700°C are listed in Table III. The dielectric properties of the materials fired to 450°C were measured as a function of temperature. Figure 11 shows the cooling curves for the uniaxially (A) and isostatically (B) pressed materials. The results show that the method of pressing the material has little influence on the properties, while firing the material decreases the strength and density, and increases the porosity of the material.

8.0 SUMMARY

A summary of the work during the second year of the project is listed below.

1. Porous SiO_2 films (porosity ~40%) ranging in thickness from 1 μm to 25 μm with k ~ 2.2 and tan δ less than 0.005 were prepared by sol-gel process. Porous colloidal SiO_2 gels of 1 mm in thickness with k from 1.6 to 2 and tan δ = 0.001 were also prepared by sol-gel process.

2. Reactively sputtered SiO_2 films of thickness 5-10 μm exhibited k ~ 3.4 and tan δ = 0.005.

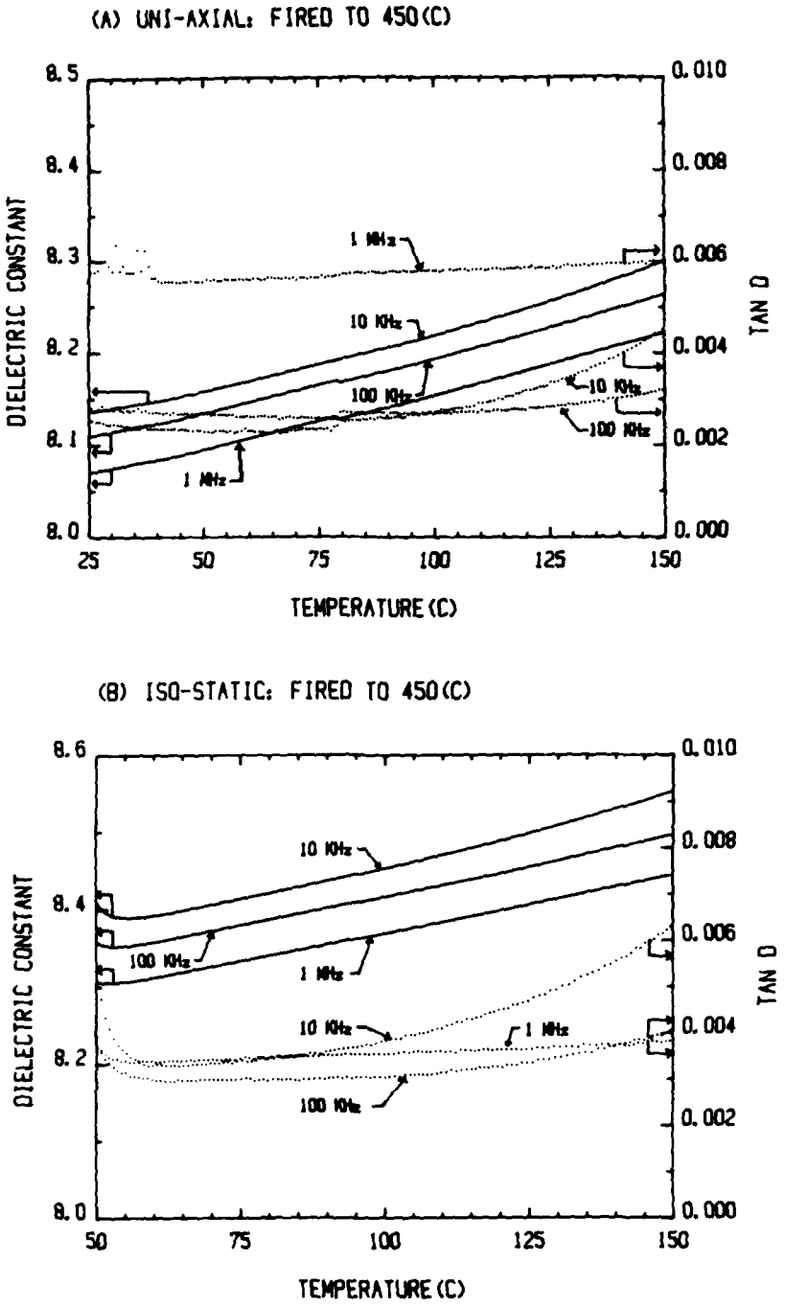

Figure 11. Relative permittivity and loss tangent vs. temperature for a) uniaxially and b) isostatically pressed silicate based cement.

Table III. Tests on Low Water-Content Cements. Firing of Uniaxially and Isostatically Pressed Materials.

Splitting Strength (psi):

	Uniaxial		Isostatic	
	Mean	Std. Dev.	Mean	Std. Dev.
Unfired	1000.2	88.2	1121.3	116.1
Fired at 450°C	960.7	127.7	954.2	105.1
Fired at 700°C	678.8	87.3	651.0	72.3

Density (g/ml):

	Uniaxial		Isostatic	
	Mean	Std. Dev.	Mean	Std. Dev.
Unfired	2.486	0.023	2.462	0.017
Fired to 450°C	2.458	0.028	2.439	0.027
Fired to 700°C	2.430	0.015	2.418	0.026

Porosity (%):

	Uniaxial		Isostatic	
	Mean	Std. Dev.	Mean	Std. Dev.
Unfired	17.66	0.39	18.07	0.55
Fired to 450°C	20.58	0.92	20.97	0.82
Fired to 700°C	21.50	0.43	21.41	0.72

3. Relative permittivity of porous vycor glass ranged from 2.6 to 3.3.

4. Calcium aluminate cement loaded with silica microballoons and prepared by MDF process had a k of 4.7.

9.0 EVOLUTIONARY STUDIES

9.1 Introduction

The following areas of study were proposed for the fiscal year 1986:

1) Select and apply various metalizing materials to the ceramic composites, and measure the physical and electrical properties after firing.

2) Reduce the particle size of the fritted raw materials to a controlled, usable size and distribution to form reproducible tapes; solve the rheologic problems and finalize the tape formulae.

3) Conduct firing studies with the aid of information gathered by TGA and DTA to determine the proper profile to eliminate internal voids, obtain optimum character and uniform density.

4) Fabricate a multilayered demonstration package utilizing the finalized tape and metalizing selections.

9.2 Results and Discussion

9.2.1 Rheology

The formation of ceramic tapes from a slurry or slip composed of several chemically different inorganic powders which vary in density and particle size distribution is difficult. These differences caused numerous rheological problems resulting in cracked tapes, gelled slip, poor release characteristics, and non-reproducible physical properties of the fired ceramic. The tape casting method of forming ceramic products is one of the most difficult means of forming ceramic products, since it is very materials sensitive. Compared to pressing or extrusion, it is hampered by the lack of corrective capabilities such as varying forming pressures.

In this method, an inorganic powder was combined with an organic binder, plasticizer and solvents to form the casting slip. Normally, the lower the solvent content the less chance of cracking during drying. Also, the lower the viscosity, the better the working properties of the slip. To accomplish the above two conditions, a low viscosity, low molecular weight binder material and a co-solvent system were selected. Unfortunately, the resultant tapes cracked on drying or were fragile after drying. Increased binder content did not eliminate the cracking problem. A second binder, in the same

chemical family but having a higher molecular weight and viscosity, was evaluated with greater success. The solvent level, however, required a thirty percent increase to impart the desired viscosity and workability to the slip.

The reduction in particle size due to milling time of the frit material had a marked effect on the rheology of the slip. The longer milling time (72 hours vs 24 hours) resulted in more problems with rheology. Since the efforts were being diluted with two compositions and two particle size ranges of frit, the longer milling period of 72 hours was eliminated. This allowed the effort to be concentrated on 24 hour milled lead borosilicate (LBS) and calcium borosilicate (CBS) frit materials.

During the early stages of the program the slip displayed a lack of stability (i.e., a change in viscosity during storage), resulting in an unacceptable condition of either thixotropy or dilatency. Tapes cast from these sips were inferior and not reproducible. The co-solvent system was changed from a methyl isobutyl ketone/ethanol (MIBK/EtOH) system to an MIBK/methanol system in a 60/40 ratio, which lowered the working viscosity considerably. The addition of surfactants, e.g. sorbitan trioleate, oxidized fatty acids, phosphate ester and ethoxylated nonyl phenol, improved the slip flow characteristic in some instances. The phosphated ester eliminated the dilatent nature of the slip but created an interfacial sticking problem between the tap and the carrier surface. Other carrier materials were investigated but the release properties were too inconsistent to warrant any changes in work direction. The oxidized fatty acid was chosen for further investigation based on its overall contribution.

In review of the solvent-binder-surfactant systems indicated, the rheological behavior and presence of rapid gelling may not be solely related to materials. A study showed that altering 1) the processing step and 2) the order of addition of the organic materials led to the elimination of the rapid

gelling phenomenon. The 24 hours milled LBS frit slips were modified initially to build up a stock of acceptable tape.

The formula used was:

Material	Weight Percent
Alumina	35.20
LBS Frit	28.80
Solvent	28.80
Binder	2.56
Plasticizer	3.20
Surfactant	1.44
	100.00

In like manner, the 24 hr milled CBS frit slips were modified to build up stock of acceptable tapes.

The formula used was:

Material	Weight Percent
Alumina	32.79
CBS Frit	26.83
Solvent	32.79
Binder	2.38
Plasticizer	2.98
Surfactant	2.23
	100.00

The improvement in the tape quality resulted mostly from changes in the milling procedure, (i.e., changing the sequence of addition of ingredients) rather than formula changes, although the formulas did receive "extra-fine-tuning" adjustments.

9.2.2 Tape Stability

Both alumina-LBS and alumina-CBS type tapes were tested for weight and dimensional stability under varying relative humidity conditions of 0, 50 and 95 percent over a 140 hour period. Both compositions had similar drying shrinkage values of approximatley 0.1 percent (.001 inches per inch) during the first eighteen hours, and remained stable beyond that time period.

9.2.3 Firing Studies

Prior to the firing of metalized packages, unmetalized, laminated 1"x1" test specimens (monitors) of each composition were fired at various temperatures and profiles to determine the optimum properties of the ceramic as noted below:

Composition	Firing Temp. (°C)	Fired Density (gms/cc)	Open Porosity (%)	Fired Shrinkage (%)
Alumina-LBS	920	3.07	0.21	9.9
Alumina-CBS	830	2.95	0.03	10.3

Although density is a function of firing temperature, it is also a function of entrapped porosity caused by poor binder removal or degasing of one of the constituents at elevated temperatures. Determination of the optimum profile can minimize these voids. It has been found that changes in rheology to improve the slurry characteristics tend to vary the degrees of firing shrinkage.

9.2.4 Test Package

The test package selected for the program was a six layer motherboard design utilizing conductive circuitry patterns on each layer and metalized vias connecting each of the circuit layers. Since this package was designed

to accommodate surface mount chip carriers, no surface cavities for chip mounting were necessary.

Vias were punched in each card with hard tooling in designated patterns for each layer. The vias were filled with conventional screening equipment utilizing metal masks. The conductor patterns were screened on the same equipment with state-of-the-art stainless steel screens.

The cards were stacked in proper sequence in a steel fixture and laminated at 250°F at 1000 psi for 120 seconds. The packages were separated out of the laminate by conventional punching techniques and by razor scoring. The packages were then fired in an air atmosphere in a computer programable kiln at 830°C and 920°C for the alumina-CBS and alumina-LBS compositions, respectively. Firing shrinkage, fired density and porosity were determined earlier for each composition through the use of monitors. The fired shrinkage of the packages, density, and porosity could not be determined directly. Unmetalized 1"x1" monitors of the same tape lots were placed in the kiln with the packages to evaluate the physical properties.

9.2.5 Metalization

In the original plan, gold, silver, platinum, palladium, nickel, and copper metals were listed as candidates to be investigated in the co-firing program. Further refinements in the selection of metals were reduced to gold, silver and copper. Silver was selected for the preliminary studies due to availability and cost, since there would be considerably metal loss involved while perfecting the application process.

Initially, two silver screening pastes from Ceronics, designated #911F and #911NF, (containing ten (10) percent and zero percent glass frit respectively), were investigated. Test patterns comprised of 0.010, 0.025 and 0.050 inch wide parallel lines were screened on cards of alumina-LBS and

alumina-CBS compositions and laminated into test specimens at 250°F at 1000 psi for 120 seconds.

After firing the above specimens at the appropriate temperatures, the #911NF silver was selected for future study due to its acceptable physical and electrical properties. The #911F silver was rejected as it blisteredon the alumina-CBS ceramic, and had a lacelike appearance and a higher electrical resistance on the alumina-LBS ceramic. The electrical properties will be discussed later in this report.

Via filling pastes usually have high metal solids contents ranging from 85-90 percent to minimize the drying and firing shrinkage effects. The initial batch of #911NF, supplied at 80 percent solids with a viscosity of 27,000 centipoise, did fill the vias as well as desired. The low solids content exhibited high shrinkage, resulting in bore coated vias rather than solid filled vias.

The second batch was supplied at a high viscosity of 44,000 centipoise and performed much better. Repeated filling cycles, with forced drying between each cycle, were necessary to achieve a solidly filled, flush via. A new batch of paste, having a 90 percent solids content, has been ordered for future work.

The changes in the paste characteristics have required modification of the squeegee mechanism, which has improved the filling quality.

In the early stages of the screening operation, many patterns were smeared or spread beyond the desired pattern form due to improperly adjusted equipment. This has been rectified through operator training and familiarization with the equipment. The remaining smears, caused by physical handling, will be eliminated by altering the paste with a hardening agent. This may decrease the incidence of electrical shorts in the fired packages.

Because the use of external silver metalization for packages does not meet with military approval, the test package has been modified by the application of gold screening paste. A Ceronics fritless gold #1160NF, having 45 percent solids, has been purchased to print the external conductor patterns. Packages containing the silver vias and gold external conductor patterns have been fabricated in both alumina-CBS and alumina-LBS type ceramics. Although the fired gold had sufficient adherence when tested with "Scotch Tape," it could not be evaluated by a soldered wire pull test since gold has poor leach resistance in 60/40 Pb/Sn solder. A fritied platinum/gold screening paste (DuPont 9885) which is fairly resistant to leaching, has been ordered. The fritted material will be used on the lead attach pads, while the pure unfritted gold will be used on the remaining conductor paths.

For some unexplainable reason, the externally screened gold blistered, cracked and peeled in varying degrees at the point of contact with the silver vias. This condition may be eliminated with the use of the DuPont fritted gold/platinum conductor paste.

A search for sources of electronic grade copper metal powder has so far yielded two suppliers, Baker Chemical and Sherritt Gordon Mines. Powders were ordered from each, but only Baker Chemical has responded to date. During the next quarter, the Baker material will be formulated into screening paste and applied to the packages. In the interim, the kiln is being adapted to fire with nitrogen atmospheres.

9.2.6 Package Firing

Earlier DTA and TGA analysis of the composite materials, in addition to increased knowledge of organic volatilization and borate chemistry aided in the design of a firing program to optimize the shrinkage and density of both compositions. The following is a representative program:

Ramp-up at 4°C min from RT to 300°C.

Hold for 20 minutes.

Ramp-up at 4°C/min. from 300-600°C.

Hold for 60 minutes.

Ramp-up at 5°C/min. from 600-830°C for CBS.

Ramp-up at 5°C/min. from 600-920°C for LBS.

Hold for 10, 20 or 30 minutes (as desired).

Turn off heat and allow to cool with or without forced air.

Earlier fired density and shrinkage measurements of packages resulted in the following data:

Composition	Firing Temp (°C)	Fired Density Monitor (gm/cc)	Fired Shrinkage (%) Monitor	Package (Length)	Package (Width)
Alumina-LBS	920	3.06	9.9	10.0	10.8
Alumina-CBS	830	2.95	10.3	10.5	9.9

The above parts were fired on MgO-coated alumina setter plates in an attempt to eliminate the sticking problem encountered on uncoated alumina setters. Since the MgO powder tended to become imbedded in the metalizing material, it was decided to investigate the effect of other setter materials. Setters composed of mullite, cordierite and zirconia were procured for continued studies. In some instances, the setters required special surface flatness machining prior to use. Unmetalized, 6 layer, 1" x 1" monitors were prepared from each composition. In the firing study, a 1" x 1" monitor and a 6-layer package of the same composition were placed on each type of setter plate and fired at the proper temperature.

Although there was evidence of reaction between the new setters and the packages, no severe sticking was encountered as with the alumina setters. The packages did require preferential orientation, with respect to which metal

pattern was in contact with the setter. CBS packages required the opposite orientation from the LBS packages. That is, one requires the top metalization pattern to be fired in the up position while the other required the same pattern in the down position. This phenomenon is related to metalization and composition rather than structure since the unmetalized 1" x 1" specimens fired flat regardless of orientation. Comparison of the physical properties of the alumina-CBS and alumina-LBS ceramics fired on the various types of setter materials with two different means of convection as displayed in Figure 1.

As reported earlier, alumina-CBS packages made with General Color and Chemical raw materials exhibit a yellow discoloration. It was theorized that the yellow color resulted from a colloidal dispersion of silver metal particles in the glassy phase. Further, it was hypothesized that the silver colloids occur from an exchange reaction between Na_2O and Ag metal, with a subsequent reduction of Ag^+ in the presence of strong reducing agents. To test this theory, various aqueous solutions were prepared and painted on the surface of packages so as to intercept lines of metalization. In the case of sodium silicate, a yellow hue was detected at the intercept, indicating that the hypothesis may be correct. The solution to this problem lies in obtaining "clean" (i.e., low sodium) fritted materials. PSU and Interamics are currently working jointly to obtain such materials.

In an effort to promote faster, cleaner burnout and decrease the presence of binder burnout products (which can act as a localized reducing agent), forced convection was employed. The comparison on Figure 1 shows that the type of convection has little to no effect on the processed package.

9.2.7 Electrical Testing

The dielectric constant and dissipation factor of alumina-LBS samples fired at 920°C and alumina-CBS samples fired at 830°C were measured at 1 MHz as listed below:

Composition	Dielectric Constant	Dissipation Factor
Alumina-LBS	7.5	.001
Alumina-CBS	7.9	.002

The earlier report of relative conductivities was in error due to the misinterpretation of data. The difference noted between the alumina-CBS and alumina-LBS are still present. It is speculated that the difference may be caused by a localized reduction of Pb^{+2} in the LBS frit to metallic lead, which alloys with the silver metalization, causing a decrease in electrical conductivity. The resistance measured on the same trace of the alumina-CBS, alumina-LBS and co-fired alumina/tungsten packages resulted in the following values:

Package Type	Resistance (ohms)	Relative Resistance
Alumina-CBS	.073	1
Alumina-LBS	.254	3.5
Alumina/W	.418	6.8

Surface insulation measurements made at 72°F/55% R.H. at 100 VDC (as per MIL-STD-883C, Method 1003, conduction D) ranged from 10^{10} to 10^{11} ohms for both alumina-CBS and alumina-LBS packages. Slightly higher values were previously reported as the result of improperly calibrated equipment.

9.3 Proposed Future

The following investigations are planned:

1) Further investigation of refractories (i.e., "setters").
2) Chemical durability testing of the packages and ceramics.
3) Initiate the exploration of revolutionary materials/processes currently under investigation.
4) Improve the via filling method and materials.
5) Fabrication, application, and firing of copper and gold metalizations.
6) Analysis of the alumina and frit materials.
7) Investigation of the chemical, physical, and electrical properties of the LBS and CBS frits.
8) Investigate other frit compositions.
9) Fine tune all rheological systems.
10) Fine tune all firing programs.

Table IV. Fired Shrinkage and Density vs. Setter Composition.
(Arranged in order of increasing values.)

Composition	Fired Package Shrinkage (%)		Test Specimen (1"x1") Fired Shrinkage (%)		Fired Density (gm/cc)	
CBS	AMg	9.7	ZF	8.3	ZF	2.89
CBS	M	10.1	CF	8.7	MF	2.90
CBS	CF	10.3	C	8.7	CF	2.90
CBS	MF	10.4	Z	8.8	Z	2.90
CBS	C	10.5	AMg	9.0	M	2.90
CBS	Z	10.8	MF	9.0	C	2.90
CBS	ZF	11.1	M	9.2	AMg	2.90
LBS	C	7.8	AMg	8.4	MF	2.85
LBS	AMg	8.4	ZF	9.0	AMg	3.00
LBS	Z	9.0	Z	9.3	ZF	3.03
LBS	M	9.2	C	9.4	M	3.06
LBS	MF	9.5	MF	9.5	C	3.07
LBS	ZF	10.0	CF	9.5	Z	3.07
LBS	CF	10.2	M	9.6	CF	3.07

Key: AMg = Alumina/MgO
M = Mullite
C = Cordierite
Z = Zirconia
F = Forced draft on heating

REFERENCES

1. A.R. Von Hippel, Dielectric Materials and Applications (MIT Press, Cambridge, 1966), p. 301.

2. J.D. Birchall, K. Kendall and A.J. Howard, U.S. Patent 4,353,748 (October 12, 1982).

3. J.D. Birchall, Proceedings of a Royal Society Discussion Meeting on Technology in the 1990's; Developments in Hydraulic Cements, Ed. P. Hirsh (University Press, Cambridge, 1983) p. 31.

APPENDIX I

To be published in the Proceedings of 1986 MRS Spring Meeting held in Palo Alto, CA.

ULTRA-LOW DIELECTRIC PERMITTIVITY CERAMICS AND COMPOSITES FOR PACKAGING APPLICATIONS

L.E. CROSS AND T.R. GURURAJA
Materials Research Laboratory, The Pennsylvania State University,
University Park, PA 16802

ABSTRACT

To accomplish the interconnect systems which will be required in the next generation of very high speed Ga:As digital ICs, it will be necessary to use strip line techniques for signal traces which must be deposited over very low permittivity dielectric substration. Materials with relative dielectric permittivities k < 3.0 and very low loss tangent up to microwave frequencies will be required. For ceramic systems such values are impossible to achieve in single phase monoliths, and composite approaches are required. Techniques for processing ceramic insulators which permit the introduction of controlled pore structures are discussed. The introduction of pores degrades some other desirable properties of the ceramic such as mechanical strength and thermal conductivity so that control of both scale and location of pores is desirable.

Materials investigated include sol-gel processed silica films and monoliths, reactively sputtered silica, etched glass compositions and Macro-Defect-Free (MDF) cements.

INTRODUCTION

A current "state of the art" approach for electronic packaging of silicon integrated circuits (IC) is the thermal conduction module (TCM), fabricated from multiple tape cast alumina ceramic layers using molybdenum or tungsten metallization for interconnections [1]. However, the evolving demands of very large scale integration (VLSI) will require even more sophisticated interconnect circuitry on the substrate [2]. A very important property of the substrate material for microelectronic packaging in the light of increasing switching speeds of transistors is its dielectric permittivity. The dielectric permittivity of the substrate governs the time delay (T_d) of the signal according to the equation $T_d = (k)^{1/2}\ell/c$, where k is the relative dielectric permittivity (dielectric constant), ℓ is the distance the signal travels, and c is the speed of light [3]. In current packaging technology with high permittivity alumina (k ~ 9-10), the delay introduced in the package exceeds the chip delay. To meet these delay considerations, there is an urgent need to reduce the permittivity of the substrate below that of alumina. Secondly, the characteristic impedance of the signal line also depends on the relative permittivity of the ceramic, as well as the density of wiring. The impedance is equal to the square root of the ratio of the inductance per unit length to capacitance per unit length. By lowering the k, the thickness of the layers can also be reduced, thereby allowing even thinner layers for the same impedance [3].

Another requirement in microelectronic packaging that needs to be addressed at this point is to decrease the line resistance associated with tungsten or molybdenum metallization which are the only metals that can be cofired at the high temperatures required for alumina. A reduction in the processing temperature to less than 900°C will facilitate the use of alternate metallurgy such as Cu, Ag or Al.

An even more compelling urgency to consider new materials, composites, and fabrication techniques for the substrate and mounting structures becomes evident when one considers the rapidly evolving Ga:As IC

technology. In Ga:As ICs, the very high switching speeds (t_s < 100 ps) combined with lower density of circuits/chip places even more stringent requirements upon stripline interconnect designs. Studies by Gilbert [4] at Mayo Clinic have shown that for packaging high speed Ga:As VLSIs, the upper limit of k is 3. From impedance calculations using a value of k = 3, the minimum substrate thickness works out to be 25 microns.

There are a number of organic polymer materials with very low relative permittivity (k < 2.5). However because of stability problems posed by organics, particularly in radiation environment, our effort has been to develop ceramic-based materials with ultra-low permittivity.

Evaluation of possible inorganic materials with low permittivity indicates a lower limit for single phase materials of order 3.8 in silica glass. Thus it is not possible with existing single phase inorganic dielectrics to achieve this very basic requirement of ultra-low permittivity, and a composite approach involving at least one much lower permittivity phase will be essential.

In the approaches taken in our investigation, the second phase has been chosen to be gas or vacuum phase with k = 1. The focus has been to develop tractable low permittivity inorganic host dielectrics with controlled pore structure. Although a viable substrate for packaging VLSIs has many other important parameters such as mechanical strength, thermal conductivity, etc., which should be considered, the primary goal of our research was to develop ultra-low permittivity dielectrics. In this regard, several processing techniques have been explored to prepare ceramic/void nanocomposites with ultra-low permittivity. In the subsequent sections, experimental procedure and results of our initial work on four topic areas listed below will be described: The advantages and limitations of the different processing routes will also be mentioned. The four topic areas are:

1. Sol-gel processing of SiO_2 films and monoliths.
2. Sputter deposited SiO_2 film structures.
3. Microporous glass structures.
4. Macro-Defect-Free (MDF) cements.

DIELECTRIC MIXING RULES

The basic approach which has been used for lowering k is that of "mixing" with dielectric ceramic pores of controlled geometry which contain air or inert gas with k close to unity. A general question which must be addressed here is the mode of interconnection between the two phases and its effect on the dielectric properties. Since the introduction of pores is associated with a sacrifice in mechanical strength, it is preferred to use a mode of mixing which would keep the volume of the void space as small as possible consistent with achieving the needed level of permittivity.

A listing of four simple dielectric mixing rules are presented in Table 1, in which the effective permittivity of the composite is represented as a function of volume fraction of relative permittivities of the two phases [5]. A graphical representation of these mixing rules using SiO_2 glasses and air with k of 3.8 and 1, respectively, is given in Figure 1.

In parallel mixing, the dielectric is in the form of a room and pillar structure with columns of dielectric dominantly parallel to the electric field. In series mixing, layers of the two phases are stacked alternately with E-field normal to the layers. The series mode is clearly more advantageous in reducing the permittivity but obviously difficult to realize in practical structure. For a composite dielectric in which neither parallel nor series mixing is strongly preferred, i.e. systems with random connectivity, the empirical Lichtenecker's logarithmic mixing rule is often applied (Table I, Figure 1). In the case where small spherical

Table I. Dielectric Mixing Rules for Two Phase Composites [5].

$\frac{1}{K} = \frac{V_1}{K_1} + \frac{V_2}{K_2}$	$K = K_1V_1 + K_2V_2$
a) Series Mixing	b) Parallel Mixing
$\ell nK = V_1 \ell nK_1 + V_2 \ell nK_2$	$K = \frac{V_2K_2(\frac{2}{3} + \frac{K_1}{3K_2}) + V_1K_1}{V_2(\frac{2}{3} + \frac{K_1}{3K_2}) + V_1}$
c) Lichtenecker's Logarithmic Mixing	d) Maxwell's Mixing

K = average relative dielectric permittivity.
K_1, V_1 = relative dielectric permittivity and volume fraction of phase one.
K_2, V_2 = relative dielectric permittivity and volume fraction of phase two.

pores are uniformly distributed in the matrix phase, Maxwell's mixing rule is applicable.

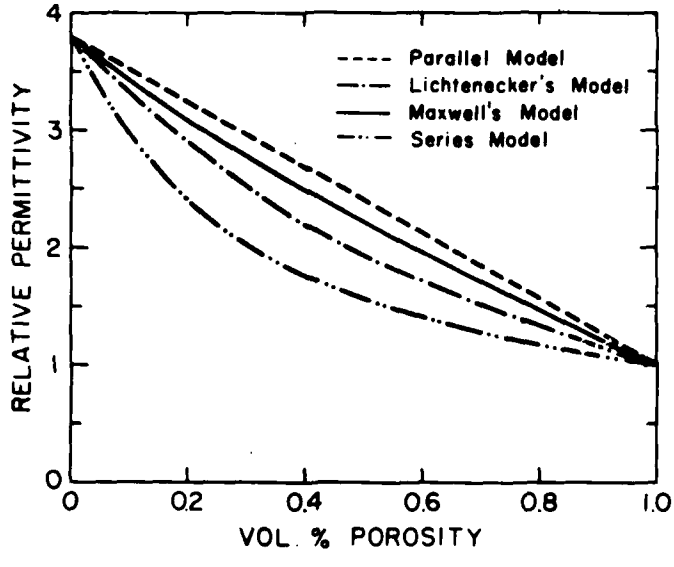

Figure 1. Relative permittivity of porous silica glass as a function of volume percent porosity for series, parallel, Maxwell's and Lichtenecker's mixing rules.

It should be noted in all the above calculations, an assumption is made that the composite feature is small compared to the wavelength. Even for 10 GHz frequency components, the wavelength is of the order of 1.5 cm in a material with k of 4. Clearly this dimension is very much larger than the scale of any of pore structure envisaged, so these simple calculations provide an initial guide for selecting pore volumes which will be required for any given host permittivity and architecture.

SOL-GEL PROCESSING OF SiO_2 STRUCTURES

The objective of the sol-gel processing SiO_2 was two fold. 1) To develop a method to spin cast 1 to 25 micron thick films of porous SiO_2. 2) To explore the possibility of forming colloidal SiO_2 gels which are thick enough to support multilevel wiring.

Thick Film Coatings of Porous SiO_2

Flow chart for processing of sol-gel derived SiO_2 thick films is presented in Figure 2. A commercial Ludox AS-40 sol (DuPont, Wilmington, DE) was mixed with 3 weight percent PVA solution in water. The viscosity of the solution was allowed to increase through the evaporation of water. When the viscosity reached 10-100 poise, the solution was applied on a low resistivity (0.001-0.006 ohm-cm) silicon substrate (Pensilco Corp., Bradford, PA) and spun at 2000-3000 rpm for 5 minutes. The film was dried in open air for 12h to allow shrinkage through evaporation of water and then dried at 100°C to get rid of residual water present. The polymer network provides the mechanical strength to the colloidal gel during the drying process thereby overcoming the cracking behavior. The film was heated at the rate of 2°C/min to 500°C and held there for about 1h. Even temperatures as low as 350°C could be used for firing if a continuous flow of oxygen is used in the furnace. The thickness of the films ranged from 1 to 25 microns depending on the viscosity of the solution. The thickness of the films were measured using both a profilometer and a scanning electron microscope.

Samples were prepared for permittivity measurements by sputter coating a 1 inch diameter gold electrode on the SiO_2 film. The back surface of the low resistivity silicon wafer served as the other electrode. Low frequency (100 Hz to 100 kHz) capacitance and loss tangent of SiO_2 films were measured using HP multifrequency LCR meters (Models 4274A-A, 4275-A) in the temperature range of -50 to 100°C. The relative permittivity and loss tangent of a representative sample are plotted in Figure 3. The relative permittivity was approximately 2.2 with loss tangent below 0.005 up to 100°C. The dissipation factor was found to be below 0.03 even after exposing SiO_2 films to humid atmospheres for over two weeks.

A wavelength scanning ellipsometer (Sopra, Bois-Columbus, France) was used to determine the porosity in SiO_2 films and it was found to be approximately 40%. From the Figure 1, it can be seen that the estimation of effective permittivity using Lichtenecker's random mixing model with 40% porosity agrees well with the measured k of 2.2.

Thus, this process gave both the required thickness and also the appropriate dielectric properties specified for packaging Ga:As ICs. Dielectric measurement on these films in the GHz frequency range are being performed. It should be mentioned here that the ability to process the films at 350°C is an added advantage of this technique.

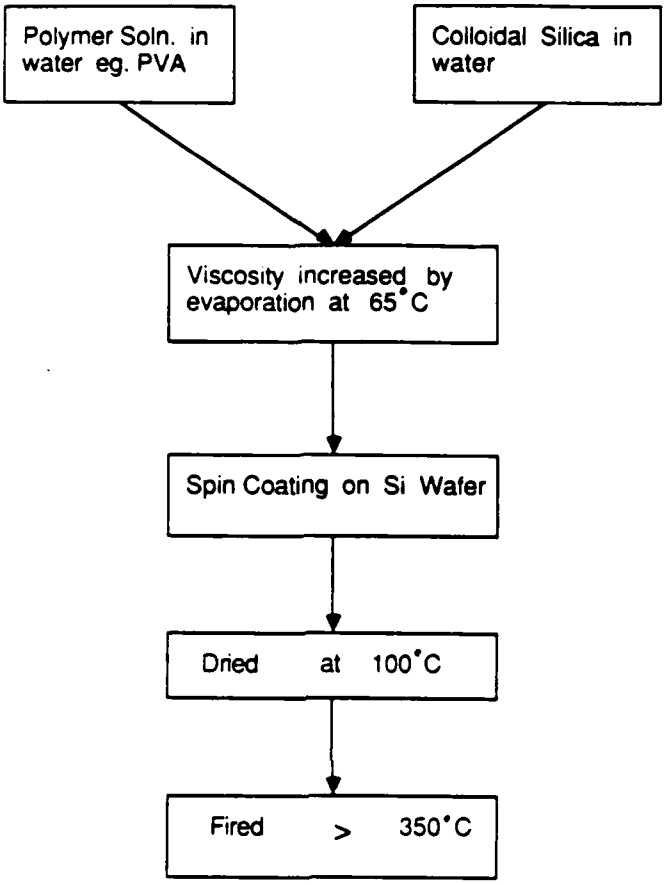

Figure 2. Flow chart of processing of sol-gel derived SiO_2 films (thickness = 1-25 μm).

Colloidal SiO_2 Gels

In this method, Cab-O-Sil L90, a relatively low surface area (~90 m^2/g) fumed silica containing <2 ppm Na_2O (Cabot Corp., Tuscola, IL) was used to prepare a colloidal sol in water. This could be readily prepared by dispersing in high shear rates at solid levels of ~20 weight% using either acidic or basic stabilization, i.e., at pH levels of ~3 or 9-11. The acidic sol was metastable as prepared and formed a weak gel at long standing (2-3 months) at room temperature. The basic sol was stable indefinitely.

Xerogels were prepared from such sols by two different methods. In the simplest case, a xerogel was obtained by slowly evaporating the liquid. Samples suitable for dielectric measurements could not be obtained this way as significant amounts of warpage and fracture usually result from the large tensile stresses developed at the surface during drying. An alternative method was to get this sol by adjusting the pH to near neutral which causes the formation of a stiff gel. This gel is then pressed into a pellet using porous media (e.g. graphite) above and below in a 2.54 cm I.D. steel pellet press. Most of the free fluid volume is removed in this step,

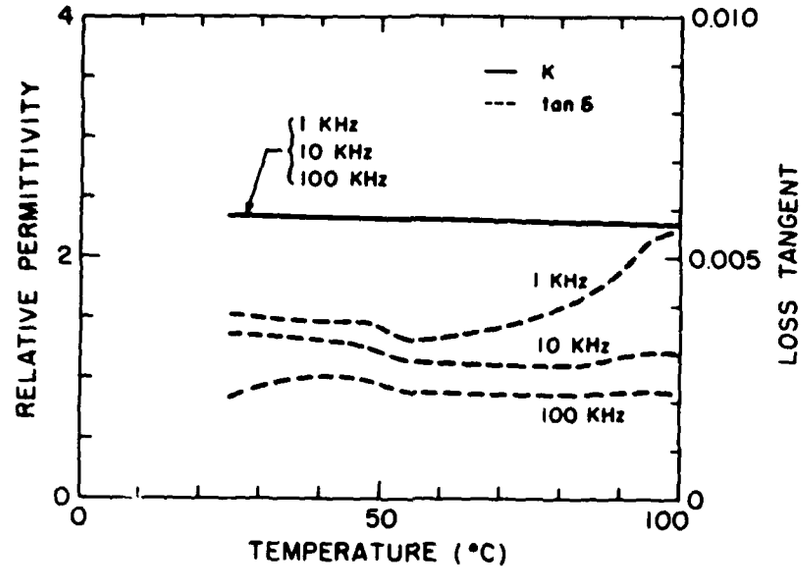

Figure 3. Relative permittivity and loss tangent as a function of temperature of sol-gel derived SiO_2 films.

which results in a gel body of sufficient integrity to resist further shrinkage on drying.

The resulting gel pellets were dried in air at room temperature for 16-24h and then fired to temperatures varying from 900°C to 1200°C for periods varying from 2 to 12h. Firing at 900°C for 12h in air was sufficient to produce a very lightly sintered xerogels of 55 to 65 volume% porosity. There is little or no shrinkage of the body below 1000°C. These firing conditions (900°C for 12h) produced a body of sufficient mechanical integrity to permit polishing and application of electrode.

Pellets of thickness close to 1 mm were prepared for dielectric measurements by sputter coating gold electrodes on either side. The measurements were performed as described earlier. The relative permittivity of porous colloidal SiO_2 gels were found to be in the range of 1.6 to 2.0. The Lichtenecker's random mixing rule, using the estimated pore volume in the gel, gives an excellent agreement to the data. The dielectric loss tangent in the samples was found to be extremely low in the range of 0.001.

SPUTTER DEPOSITED SIO_2 FILMS

In this study, RF sputtering technique was used to generate porous SiO_2 films. Since the deposition rate using SiO_2 as the target material is known to be very slow (approximately 0.12 micron/h), it becomes impractical to generate 25 micron thick films using this method. Two alternate approaches have been investigated.

In the first approach, uniform 25 micron thick amorphous Si films were first deposited. The morphology of these films were columnar, with the column diameter varying from 0.1 to 0.3 microns. This columnar structure was then anisotropically etched using the faster etch rates of the low density regions between the columns as compared to the columns themselves. Two etching techniques, one wet (chemical) and the other dry (reactive ion etch), were attempted. The etched films were thermally oxidized in dry O_2 at 1100°C. Etching out the regions around the columns would enable the

oxidation to proceed laterally into the columns rather than down the columns. Etching step was also used to introduce porosity into the films.

A limitation of this approach was encountered during the thermal oxidation due to the tremendous volume expansion as the Si-Si bonds are broken and Si-O bonds are formed. This led to severe cracking in the films. Because of this difficulty, an alternate route was investigated to prepare porous SiO_2 films.

In the second approach, the method of reactive RF sputtering of SiO_2 was used. RF reactive sputtering utilizes the benefit of higher sputtering yield of silicon and avoids an additional step of oxidation after sputtering. The dependence of deposition rate and porosity of the films on the partial pressure of O_2 and argon can be used to tailor the morphology of SiO_2 films [6].

For reactive sputtering, a 5" Si (99.99% purity) was used as the target in the RF sputtering unit (MRC model SCS8632). Three different gas pressures were selected: (a) P_{AR} = 27 mtorr and P_{O2} = 3 mtorr (10%), (b) P_{AR} = 37 mtorr and P_{O2} = 3 mtorr (7.5%), (c) P_{AR} = 44 mtorr and P_{O2} = 1 mtorr (2.2%). The RF power was maintained at 120 watts and the substrate target distance was 3.5 cm in all the cases. The films were deposited on 2.54 cm diameter low resistivity (0.001-0.0006 ohm-cm) p-type Si wafers.

The dielectric measurements were performed on the films as explained earlier. Figure 4 shows the relative permittivity as a function of temperature for the three deposition conditions. As the total pressure in the system is increased, more porosity is introduced and the permittivity is reduced. High pressures are being investigated which should decrease the permittivity further to the desired value of 3. The loss tangent were found to be less than 0.005 in all the films.

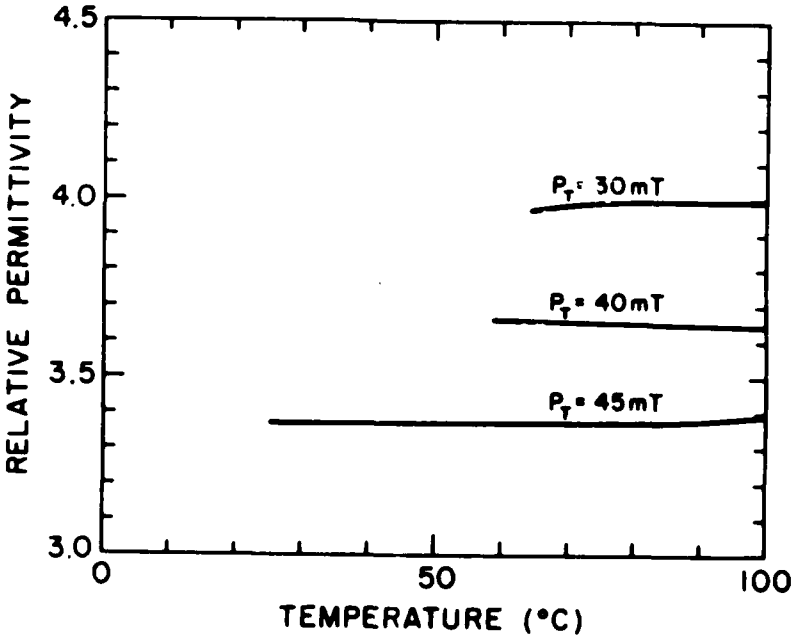

Figure 4. Relative permittivity vs. temperature of reactively sputtered SiO_2 films (P_T is total gas pressure in mtorr).

Sputter deposited porous SiO_2 films were found to absorb moisture when exposed to humid atmospheres over extended lengths of time. The films were capped with high density silica using the standard sol-gel process of hydrolysis and polymerization of tetraethylorthorsilicate [7]. Further details of the sputter deposited SiO_2/void nanocomposites could be found in an accompanying paper in the proceedings [8].

MICROPOROUS GLASS STRUCTURES

The focus in this study was to take commercially available Corning 7930 porous vycor glass and to investigate the dielectric properties in the microwave region of both as-received and leached porous structures [9]. The average pore diameter in this material is approximately 40A° so that electroding by sputtering or evaporation is not a problem.

Measurements of permittivity and loss tangent over the frequency range from 4 kHz to 10 MHz at temperatures from 25 to 125°C show excellent low permittivity (3.5) and loss tangent (0.005). To lower the permittivity a little further, a post leaching with 2 and 10% HF was tried for times of one and five minutes. After leaching, the porous vycor samples were soaked in boiling HCl to eliminate any impurities, cleaned in deionized water, and heat treated at 300 to 700 for 4 hrs in flowing oxygen. Dielectric measurements at 2.5 GHz were performed on HF treated and untreated porous vycor glass using resonance perturbation technique in a re-entrant cavity. The technique is based on measuring the change in the impedance of the cavity with the introduction of the sample. A block diagram of the equipment is shown in Figure 5.

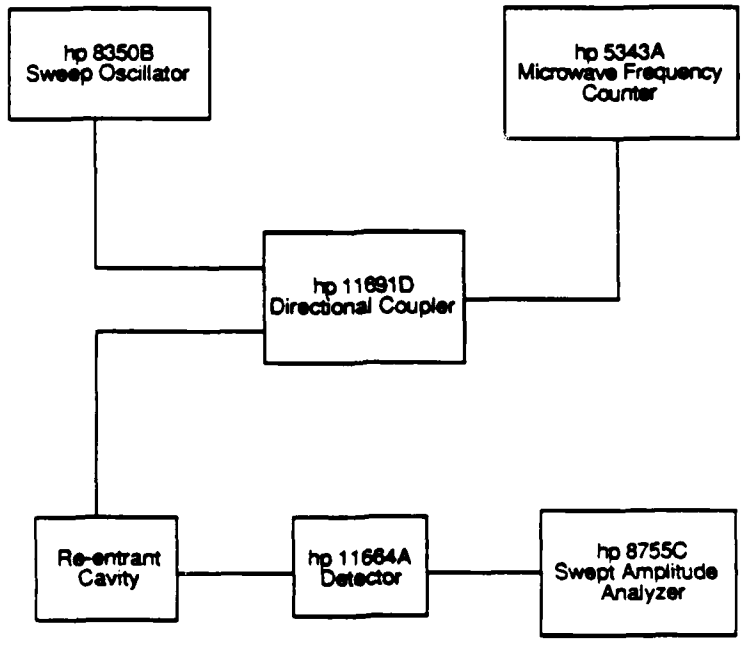

Figure 5. Schematic diagram of microwave dielectric measurement set up.

Figure 6 shows the effect of leaching and heat treatment on dielectric permittivity. From the figure, it can be observed that k of unleached

microporous silica was reduced with increasing soak temperatures reaching a minimum of 2.6 at 700°C, with loss tangent below 0.001. The heat treatment was shown to be effective in removing moisture and impurities absorbed in the glass. The relative permittivity of the 2% HF leached sample was lower than the untreated glass over the entire temperature range. The 10%HF leaching did not show any reduction in the permittivity over the untreated glass, which may be attributed to the collapse of the silica structures.

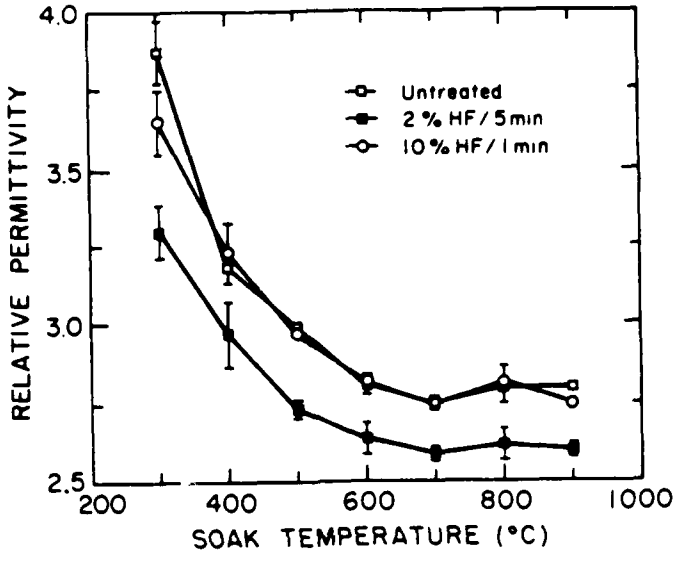

Figure 6. Effect of leaching and heat treatment on relative permittivity of porous vycor glass.

MACRO-DEFECT-FREE CEMENTS

Rationale for initiating studies in this area of chemically bonded ceramics for substrate application are (i) In the chemical consolidation process of cement curing, there is a change of phase to a hydrated form which is of lower density than the parent powder. Thus it is in principle possible to obtain full mechanical integrity without shrinkage. Since for most ceramic systems, it is the reproducibility and control of shrinkage which limits wiring resolution and density. Zero shrinkage could be most valuable. (ii) The very low temperature curing of cement permits a wide range of techniques for introducing a second phase such as hollow glass microspheres or a fugitive phase which can be lost in subsequent processing to produce the controlled pore structures which are necessary for permittivity control. The low temperature processing also permits the use of high conductive metals for interconnects.

However, a major disadvantage of cement is their inherent large porosity. Bulk mechanical properties can be related to porosity and thus it is a key factor in controlling the ultimate strength of a cement. One approach to increasing the mechanical strength of a cement is based on eliminating all but the fine porosity ($<10\ \mu$) to produce macro-defect-free (MDF) cement. The recent work of Birchall and co-workers indicates that cement produced by MDF processing has superior mechanical properties over conventionally processed cement [10-11]. Larger pores can be eliminated by reducing the water:cement (w/c) ratio ($\lesssim 0.20$) and through the use of

conventional ceramic processing (shear mixing, extrusion, die pressing, calendering).

In the first part of the investigation, commercially available calcium aluminate cements were processed by the MDF method to evaluate their dielectric properties for substrate applications. Later one type of cement was loaded up to 70 volume% with hollow glass microspheres to study the effect of controlled pore structure on permittivity. A brief report of the study is presented here. Further details are published elsewhere [12,13].

Several types of commercial calcium aluminate cements supplied by Lone Star Lafarge, Inc. (Norfolk, VA) and ALCOA (Pittsburgh, PA) were investigated. The Lone Star Cements are classified as a SECAR™ cement followed by a number depicting the weight percent Al_2O_3 content. All the ALCOA cements had approximately 80 weight percent of Al_2O_3. Samples were prepared by hand mixing 50 gm of cement in 11.11 gm of 11 wt% PVA solution resulting in a water to cement ratio of 0.20 and a PVA/(water and cement) of 0.018. The dough was then homogenized and trapped air removed by high shear mixing under vacuum in C.W. Brabender preparation mill (Hackensack, NJ). The resulting dough was prepared into 2.54 cm diameter discs in a steel die coated with teflon mold release at a pressure of 138 MPa for 10-15 seconds. Cement discs were cured at room temperature in a dessicator.

Dielectric permittivity and loss tangent measurements were performed as explained earlier with sputter coated gold electrode on either side of the discs. Typical low frequency dielectric response for calcium aluminate cement is given in Figure 7. The permittivities are quite low considering that the samples contain both unbound water and PVA. The SECAR cements show a wide range of permittivities. Permittivities for the SECAR 80 series cements are high because of their high alumina content. SECAR 71 and SECAR 60, as seen in Figure 7, have lower permittivity in the range of 4 to 6 and relatively flat frequency dependence. The dielectric permittivity of ALCOA cement with approximately 80 wt% Al_2O_3 was ~ 8, with a frequency response similar to that of SECAR 80 fast set (Fig. 7). Dielectric loss tangent in both SECAR and ALCOA cement samples were about 0.10 at 100 Hz decreasing to 0.02 at 1 MHz. In these cements cured under ambient conditions, the dominant transport of charge is the unbound water-PVA network, which is probably resonsible for the large frequency dependence of k and loss tangent up to 10 kHz.

From the above study, it is clear that the MDF processed calcium aluminate cement cannot attain the ultra-low permittivity required for packaging high speed Ga:As ICs. Therefore, introduction of closed porosity via hollow glass microspheres was considered to lower the relative permittivity of calcium aluminate cement. Although samples prepared using SECAR 60 and 71 possessed the flatest frequency response of dielectric permittivity (between 4 and 6) and therefore have the highest potential for use as dielectric substrate, SECAR 80 was chosen for this study. SECAR 80 exhibits the highest dielectric permittivity of all the cements ranging from ~13 at 100 Hz to ~7 at 1 MHz. Consequently, it is anticipated that subtle differences in the dielectric permittivity upon the addition of glass microspheres may be more pronounced in SECAR 80 as compared with SECAR 60 to 71.

High strength microballoon spheres FTD-202 (Emerson and Cuming) with an average particle diameter of 65 microns and a wall thickness of 1 to 2 microns were used in the study. Cement samples were prepared as explained earlier with microsphere loadings of 0, 27.5, 40, 50, 60 and 70 volume percent. Because of the high shear mixing, a large fraction of microballoons were destroyed during processing. Effective loading of microspheres was estimated by comparing the experimental density with the theoretically calculated densities. Microsphere loadings of 27.5, 40, 50, 60 and 70 percent were found to correspond to effective loadings of 10.6, 21.7, 10.6, 14.1 and 19.7.

The dielectric mixing rules for cement-microsphere composite, assuming relative permittivities of 6.8 and 1.17 taken at 1 MHz for the cement and

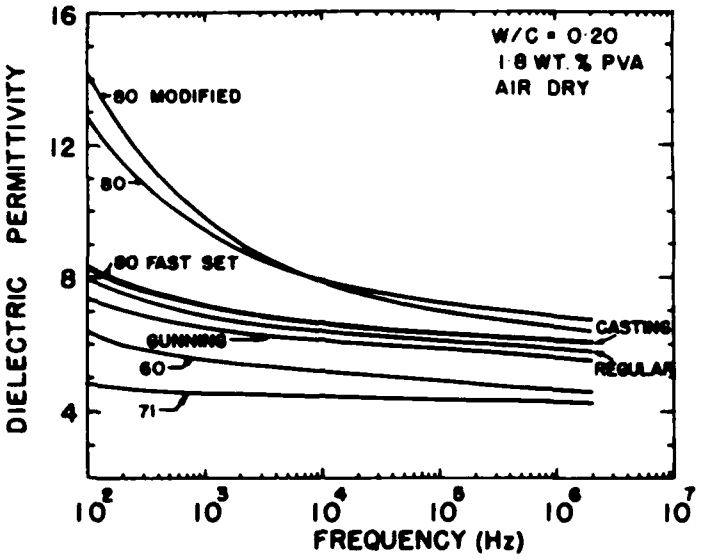

Figure 7. Relative dielectric permittivity of calcium aluminate cements containing 1.8 wt% PVA, a water-cement ratio of 0.20, cured in air as a function of frequency.

glass microspheres, are graphically represented in Figure 8. Using the relative permittivity of each composite at 1 MHz and its known effective porosity, the data for five cement-microsphere composites are plotted in Figure 8. As seen in the figure, Maxwell's as well as Lichtenecker's models are closest to the experimental data. The loss tangent for all the composites was approximately 0.02 at 1 MHz.

Thus microsphere loadings in SECAR 80 cement resulted in up to 30% lower permittivity. Application of this approach of introducing a closed pure structure into the cement could obviously be further enhanced by using a stronger microsphere or providing softer processing. Additionally, although SECAR 80 was used in this study for demonstration purposes, SECAR 60 or 71 would provide a much better baseline matrix material for further reduction of the dielectric permittivity. For example, the relative dielectric permittivity of 4.3 for SECAR 71 (at 1 MHz) would require the addition of only 30 volume percent microspheres to lower the dielectric permittivity of the composite to 2.9.

SUMMARY

A summary of the results is listed below.

1. Porous SiO_2 films (porosity ~40%) ranging in thickness from 1 μm to 25 μm with k ~ 2.2 and tan δ less than 0.005 were prepared by sol-gel process. Porous colloidal SiO_2 gels of 1 mm in thickness with k from 1.6 to 2 and tan δ = 0.001 were also prepared by sol-gel process.

2. Reactively sputtered SiO_2 films of thickness 5-10 μm exhibited k ~ 3.4 and tan δ = 0.005.

3. Relative permittivity of porous vycor glass ranged from 2.6 to 3.3.

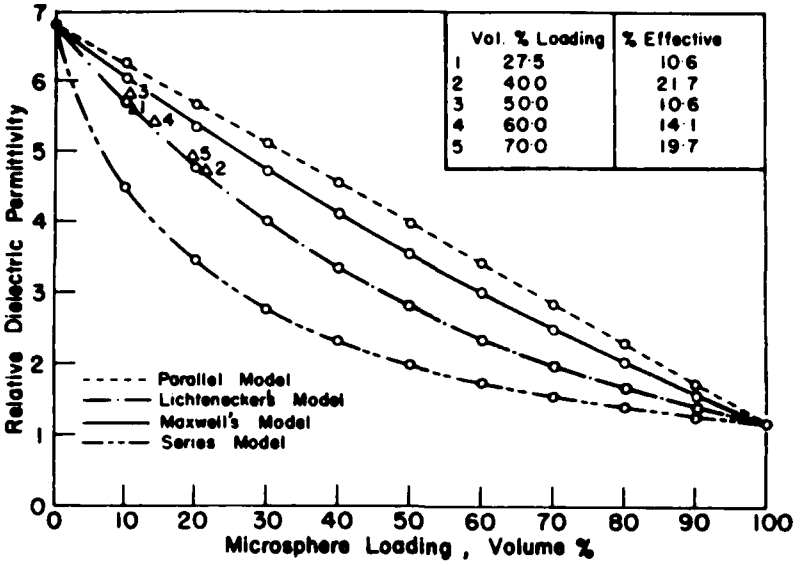

Figure 8. Relative dielectric permittivity of cement-microsphere composites as a function of volume percent microsphere loading for series, parallel, Maxwell's and Lichenecker's mixing rules.

4. Calcium aluminate cement loaded with silica microballoons and prepared by MDF process had a k of 4.7.

ACKNOWLEDGEMENTS

The work was supported by ONR contract N00014-84-K-0721 under DARPA Order No. 5157. The graduate students involved in the program are A. Das, U. Mohideen, P. Sliva, W. Yarbrough, and J. Yamamoto. A special thanks to Sharon Jows for typing the manuscript.

REFERENCES

1. A.J. Blodgett and D.R. Barbour, IBM J. Res. Develop. 26, 30 (1982).
2. D.A. Chance, Chung-Wen Ho, C.H. Bajarek, and M. Sampogna, IEEE Trans. Comp. Hybrids and Man. Tech., CHMT-5, 368 (1982).
3. B. Schwartz, Bull. Am. Ceram. Soc. 63, 577 (1984).
4. B. Gilbert (private communication).
5. A.R. Von Hippel, Dielectric Materials and Applications (MIT Press, Cambridge, 1966), p. 301.
6. A.P. Giri, Ph.D. Thesis, The Pennsylvania State University (1984).
7. S. Sakka, Treatise on Materials Science and Technology, Vol. 22 (1982) p. 129.
8. A. Das, R. Messier, T.R. Gururaja, and L.E. Cross, Proceedings of 1986 Spring Meeting of MRS on Electron Packaging Materials.
9. J.K. Yamamoto, J.H. Kim, A.S. Bhalla and R.E. Newnham (to be published).
10. J.D. Birchall, K. Kendall and A.J. Howard, U.S. Patent 4,353,748, (October 12, 1982).

11. J.D. Birchall, Proceedings of a Royal Society Discussion Meeting on Technology in the 1990's; Developments in Hydraulic Cements, Ed. P. Hirsh (University Press, Cambridge, 1983) p. 31.
12. P. Sliva, L.E. Cross, T.R. Gururaja, and B.E. Scheetz (accepted in Materials Letters).
13. P. Sliva, L.E. Cross, T.R. Gururaja and B.E. Scheetz, (submitted to Materials Letters).

APPENDIX II

To be published in the Proceedings of 1986 MRS Spring Meeting held in Palo Alto, CA.

LOW PERMITTIVITY SiO_2/VOID NANOCOMPOSITE FILMS

AMITABH DAS, R. MESSIER, T.R. GURURAJA AND L.E. CROSS
Materials Research Laboratory, The Pennsylvania State University, University Park, PA 16802

ABSTRACT

A novel approach for preparing porous SiO_2 thin films by sputter deposition is being developed. The porosity is introduced to reduce the dielectric permittivity of the film to less than 3 for potential use in packaging high speed VLSIs. In the first approach, amorphous silicon is initially deposited to produce a columnar structure with a thickness of 25μm, followed by etching and thermal oxidation to result in closely spaced SiO_2 pillars. Capping the structure by a thin film (0.1μm) silica gel layer provides the support for strip line traces. In the second approach, porous SiO_2 films are prepared by reactive sputtering. The dielectric properties of the sputter deposited SiO_2 films are presented.

INTRODUCTION

Very Large Scale Integration (VLSI) is already driving a number of new trends for mounting and packaging IC chips. A current 'State of the Art' approach is the IBM thermal conduction module (TCM), where the interconnections pass through multiple tape cast alumina substrates or planes [1]. The dielectric permittivity (k') of the substrates govern the delay in signal line interconnects [1]. Studies by B. Gilbert, et al. [2] at Mayo Clinic have shown that for packaging high speed GaAs VLSIs, the upper limit of k' is 3. Therefore there is an urgent need to decrease k' from 9.5-10.0 for alumina to 3 or below. Using a value of k'=3, from impedance calculations done by B. Gilbert, the minimum substrate thickness works out to be 25 micrometers. Although many polymeric (organic) materials have k' less than 3, because of their sensitivity to radiation, the focus of this study is to develop inorganic materials for the application. With the above criterion as a guideline along with permittivity, the logical choice is to use silica as the starting material. Silica has one of the lowest permittivities (k'= 3.8). However since the aim is to achieve k' below 3, a composite silica structure is necessary, where silica is combined with a second phase of lower k'. Since air has a permittivity around unity, the idea is to develop porous, 25 micrometer thick silica substrates. A viable substrate for packaging VLSIs has many important parameters, besides transmission delay, which should be considered, like thermal conduction, mechanical strength, crosstalk, etc. [1]. These parameters have not been dealt with in this study, and maybe handled as a part of future research.

In this study, the route for generating porous SiO_2 substrates has been by the technique of RF sputtering. In this technique, the target is bombarded with energetic ions to knock off atoms (along with some other species), which aggregate on a substrate to form a film. The deposition rate of this film depends on the target material. In the case of SiO_2 target, the deposition rate is known to be very slow [3] (approx. 0.12 micrometers/hr), hence it becomes impractical to generate 25 micrometer thick films using this method. Therefore two alternate approaches have been investigated. In the first approach, 25 micrometer thick Si films have been processed to form porous SiO_2 films. In the second approach, reactive RF sputtering has been used.

APPROACH 1

It is known that the deposition rate of Si is much higher as compared to SiO_2. Using this advantage, uniform, 25 micrometer thick a-Si films were first deposited. The morphology of these films, as shown in Figures 1 and 2 is a columnar one, with column diameters varying between 0.1 and 0.3 micrometers. This columnar structure is then anisotropically etched, using the faster etch rates of the low density regions between the columns as compared to the columns themselves. Two etching techniques, one wet (chemical) and the other dry (reactive ion etch) have been attempted. A similar etching technique has been attempted by other investigators on columnar Ge and Si films [4,5]. The next processing step was the thermal oxidation of these etched structures in dry O_2. Etching out the regions around the columns would enable the oxidation to proceed laterally into the columns rather than down the columns. Etching step was also used to introduce porosity into the films. Using the Deal and Grove model [6], for the oxidation conditions (shown later), the extent of oxidation has been theoretically estimated. In addition, an x-ray diffraction experiment has been performed to look at any crystalline phases in the oxidized films.

EXPERIMENTAL PROCEDURE

Amorphous Si films were sputter deposited using a diode RF sputtering unit (MRC Model SCS 8632). The sputtering conditions were: argon gas pressure - 30 mTorr, RF power - 70 watts, and substrate to target distance - 3 cm. The deposition rate was about 1.3 micrometers/hr. A film of thickness 25μ was deposited on single crystal Si wafers (p-type, (100) orientation). The thickness of the film was measured with a profilometer. The wet (chemical) etching procedure used a mixture of HF (40% conc.) and HNO_3 (70% conc.) as the etchant. The volume of HNO_3 and deionized water was varied from 2.5% to 15% and 2.5% to 10% respectively. The films were immersed in the etchant for 5, 10, and 15 seconds and then rinsed, using deionized water. Dry (reactive ion etching) of a-Si films was carried out at two different conditions as shown in Table I.

These etched films were thermally oxidized, using a tubular alumina furnace, through which dry oxygen (99.99% purity) was passed. The films were heated up to 1100°C. The temperature profile for the oxidation is shown in Figure 3.

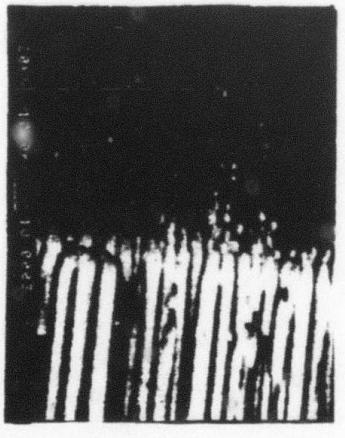

Figure 1. SEM micrograph of a fractured edge of 25 μm thick a-Si film.

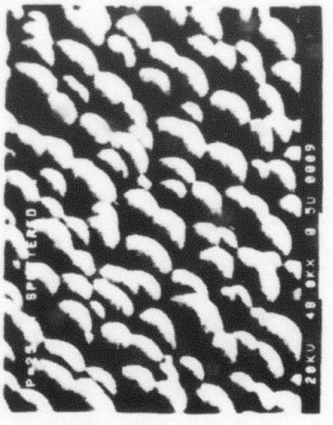

Figure 2. SEM micrograph of the top surface of 25 μm thick columnar a-Si film.

Table I. Reactive Ion Etching of a-Si Films.

Reactive Gas = NF_3, Volatile Species = SiF_4

	Etching Condition 1	Etching Condition 2
Flow NF_3 =	16 SCCM*	16 SCCM
Flow Ar =	6 SCCM	6 SCCM
Power =	650 watts	350 watts
P_{total} =	20 mtorr	18 mtorr
Time =	3 mins	3 mins
T_s =	27°C	27°C

*SCCM = Standard Cubic cm/min.

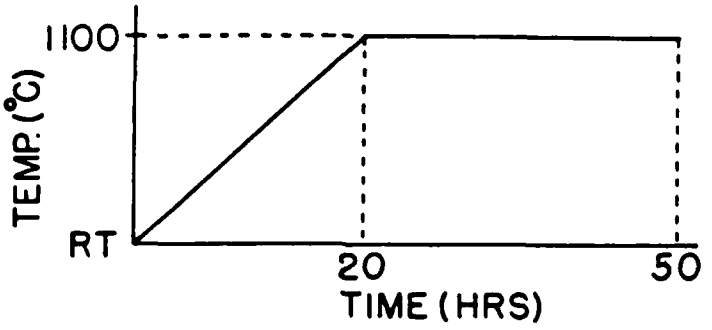

Figure 3. Oxidation temperature profile for etched Si films.

RESULTS AND DISCUSSION

Controlling the deposition conditions, it is possible to generate uniform columnar 25 micrometer thick Si films. Anisotropic etching of these films to remove the low density regions between the columns is a quick and complex process. In the case of chemical etching, the HNO_3 oxidizes the lower density regions in between the columns faster than the columns and the HF then reacts with the oxide and removes it. As seen in Figure 4 (a) and (b), because of the high aspect ratio of these columns, they seem to lose mechanical strength and lean on one another, forming clusters. In addition, it is observed that the clusters seemed to be coated with a reaction products, which occurs because of the following reaction:

$$18HF + 4HNO_3 + 3Si \rightarrow 3H_2SiF_6 + 4NO + 8H_2O.$$

In the case of the reactive ion etched films, little anisotropic etching was observed (Figs. 5 and 6) from either of the two conditions mentioned in Table I. As Si oxidizes to SiO_2, a tremendous volume expansion is known to take place as the Si-Si bond are broken and Si-O bonds form [7]. This is observed in the oxidation of the etched films (see Fig. 7).

The Deal and Grove model [6] was used to study the lateral diffusion of oxidizing species into the Si columns for the temperature profile shown in Figure 3. Taking the time of oxidation to be 40 hrs and the temperature 1100°C, the total oxide thickness is given by the following parabolic oxidation law:

$$x_o^2 = Bt$$

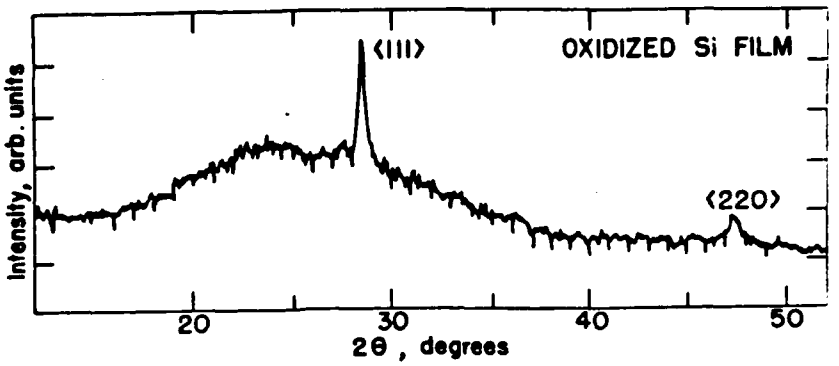

Figure 8. X-ray diffraction pattern of oxidized Si film.

APPROACH 2

Reactive RF sputtering of SiO_2 has been known for a long time. Investigations found this method of preparing SiO_2 to have a high p-etch rate [8], and therefore was found unacceptable for making gate oxides for MOSFET devices. p-etch rate or selective etch rate is often used as an indicator of the porosity of thin films. Since the interest in this study is to generate low permittivity films, the method of RF reactive sputtering was used. RF reactive sputtering utilizes the benefit of higher sputtering yield of Si and avoids an additional step of oxidation after sputtering. The dependence of deposition rate and porosity of the films on the partial pressures of O_2 and Argon can be used to tailor the morphology of SiO_2 films [9,10].

EXPERIMENTAL PROCEDURE

For reactive sputtering, a 5" Si (99.99% purity) was used as the target in the RF sputtering unit (MRC mode SCS8632). Three different gas pressures were selected: (a) P_{Ar} = 27 mtorr and P_{O_2} = 3 mtorr (10%), (b) P_{Ar} = 37 mtorr and P_{O_2} = 3 mtorr (7.5%), (c) P_{Ar} = 44 mtorr and P_{O_2} = 1 mtorr (2.2%). The RF power was maintained at 120 watts and the substrate target distance was 3.5 cm in all the cases. The films were deposited on 2.54 cm diameter low resistivity (0.001-0.006 ohm-cm) p-type Si wafers. The thickness of the deposited films were between 5 and 7 micrometers. Sputtered gold was used as the electrode for dielectric measurements. Using a HP 4274A multi-frequency LCR bridge, the k' and dielectric loss was measured at 1, 10, 100 kHz frequency as a function of temperature on cooling from 100°C to 25°C.

RESULTS AND DISCUSSION

Figure 9 shows the dielectric permittivity as a function of temperature for the three deposition conditions. Figure 10 is an indication of the average dielectric losses in these films. As the total pressure in the system is increased, more porosity is introduced and the permittivity goes down. Higher pressures are being investigated which should decrease the permittivity further to the desired value of 3. An ellipsometric technique is being used to study the effect of pressure on the porosity in the films. The dielectric losses were found to be low (less than 0.5%) in all these films.

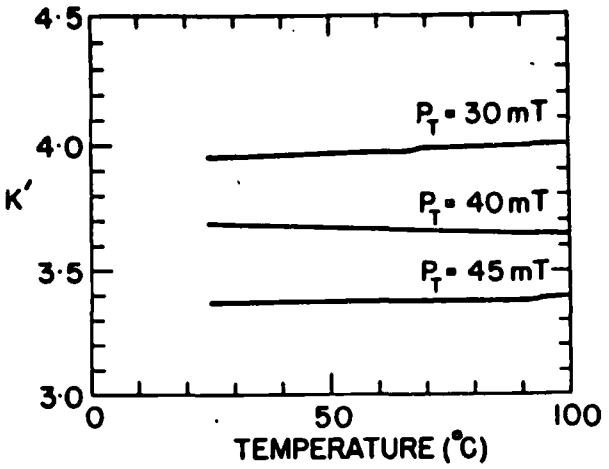

Figure 9. Dielectric permittivity vs temperature for reactively RF sputtered films.

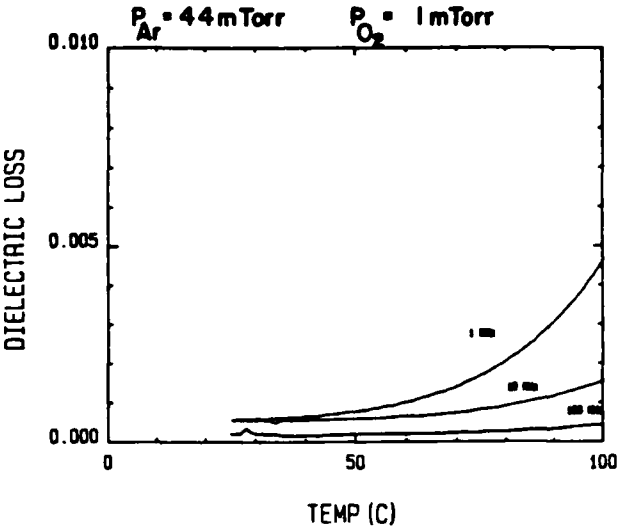

Figure 10. Dielectric loss vs temperature for the reactively RF sputtered films. P_{Ar} = 44 mtorr, P_{O2} = 1 mtorr, P_T = 45 mtorr.

SOL-GEL CAPPING

Sputter deposited porous SiO_2 films were found to adsorb water when exposed to humid atmosphere over extended lengths of time. Therefore, a sol-gel capping of these films is being investigated.

EXPERIMENTAL PROCEDURE

A standard procedure, involving the hydrolysis and then polymerization of TEOS [11] is being used. Table II shows the composition of the starting materials used. These have been stirred in a beaker at room temperature for 2 hrs. Then the films were dip coated and left to dry for about 10 hrs., after which they were heated at 350°C for 12 hrs.

RESULTS

The dip coating was attempted on 20 μm etched Ge films. Figure 11 shows the top surface of the etched film and Figure 12 is a side view of the capped film. The SEM micrographs show that the sol does not penetrate down the columns but due to surface tension, spreads over the surface of the film. Further investigations are being attempted on different porous SiO_2 films.

CONCLUSIONS

Anisotropic etching of the columnar Si structure with aspect ratios ranging from about 80 to 250 cause the columns to cluster together. This prevents complete oxidation of the film. In addition, the large volume expansion during oxidation of Si to SiO_2 would decrease the porosity considerably. This volume expansion has been estimated to be about 130%. At present, reactive sputtering appears to be a viable process for preparing porous SiO_2 films of low dielectric permittivity.

Table II. Composition of Precursors Used for Sol-Gel Capping

TEOS	2.8 vol%
Ethanol	94.6 vol%
D.I. Water	2.4 vol%
HCl	0.2 vol%

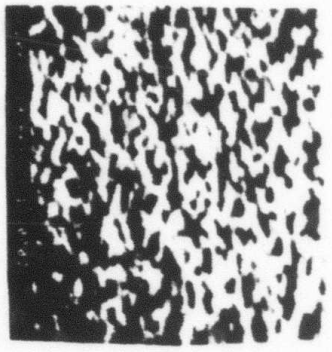

Figure 11. SEM micrograph of top surface of an etched Ge film.

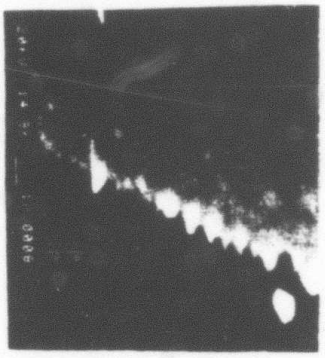

Figure 12. Side view of sol-gel capped, etched GE film.

REFERENCES

1. A.J. Blodgett, Jr., Scientific American, Sept. 1983, p. 86-97.
2. Personal communications with B. Gilbert.
3. I.H. Pratt, Solid State Technology, December 1969, p. 49-57.
4. L.R. Gilbert, et al., Thin Solid Films, 54 (1978), 149-157.
5. R. Messier, et al., J. Appl. Phys., 51 (3), March 1980, p. 1611-1614
6. Deal and Grove, Jpn. J. Appl. Phys., 36, (1965), p. 3370.
7. L.E. Katz, Chapter 4 in VLSI Technology, Edited by S.M. SZE, McGraw-Hill Publishing Co. (1983).
8. W.A. Pliskin, J. Vac. Sci. Technol. 14 (5) (Sept./Oct., 1977).
9. R.M. Valetta, et al., Electrochem. Technol. 4 (1966), p. 402-406.
10. A.P. Giri, Ph.D. Thesis (1984), "Non-Uniform Physical Structure Model for Understanding the Electrochromic Behavior of Tungsten Oxide Thin Films," The Pennsylvania State University, University Park, Pa.
11. Sumio Sakka, Treatise on Materials Science and Technology, Vol. 22, (1982), p. 129-167.

APPENDIX III

Accepted for publication in Materials Letters.

MACRO-DEFECT FREE PROCESSING AND LOW FREQUENCY DIELECTRIC RESPONSE OF CALCIUM ALUMINATE CEMENTS

PAUL SLIVA, L.E. CROSS, T.R. GURURAJA AND B.E. SCHEETZ
Materials Research Laboratory, The Pennsylvania State University,
University Park, PA 16802, USA

Abstract

Eight commercial grade calcium aluminate cements were prepared macro-defect free by high shear mixing, lowering the water/cement ratio and using polyvinyl alcohol as a plasticizer. Samples for dielectric measurements were prepared by die pressing to form disks. Relative dielectric permittivity and dissipation factor were measured over the frequency range of 100 Hz to 1 MHz. Variations in frequency response and loss mechanism between the cements is related to bulk chemistry.

Introduction

There is considerable effort being placed on the development of new low permittivity inorganic dielectrics for use with high speed GaAs integrated circuits (IC). The enhancement of material properties necessary for dielectric substrates is motivated by the more stringent requirements of GaAs IC packages. The demands of VLSI will require a higher density of interconnect circuitry, a decrease in the line resistance inherent to molybdenum or tungsten metallization and a greater efficiency of interconnects and signal wiring that limits signal propagation. Consequently, there is an immediate need to both reduce the dielectric permittivity of the substrate from that of alumina (~9.5-10) to as low as possible (<3.5) and to decrease the processing temperature below that required for alternative metallization such as silver (~900°C).

An approach to producing low permittivity substrates is through the use of hydraulic cements. Cements densify and gain strength at ambient temperature by a hydration reaction; a chemical bonding of the cementitious

grains. Densification is achieved because of the reactivity of the cementitious grains in aqueous solution and their ability to produce (a) chemically different phase(s) that hold the matrix together. Of the many types of commercial hydraulic cements available, this investigation will consider only calcium aluminate cement (also called High Alumina Cement or HAC).

Commercial grade calcium aluminate cement is produced by fusing together limestone and bauxite to form a calcium aluminate slag which when cooled is ground to a fine powder. Several cementitious phases are formed by this process including $CaAl_2O_4$ and $CaAl_4O_7$ with the major constituent always being $CaAl_2O_4$. (An alternative method of cement nomenclature divides the compound into its appropriate oxides and labels each oxide with a conventional abbreviation: CaO = C, Al_2O_3 = A, SiO_2 = S, Fe_2O_3 = F and H_2O = H. Thus $CaAl_2O_4$ becomes $CaO{\cdot}Al_2O_3$ or CA and $CaAl_4O_7$ becomes $CaO{\cdot}2Al_2O_3$ which is abbreviated CA_2). Figure 1 shows the silica deficient side of the lime-alumina-silica system [1]. Areas containing the composition of portland cements, ordinary high alumina cements and special white high alumina cements are marked P, HAC and WHAC, respectively. As can be seen from the diagram, minor quantities of other calcium aluminate phases may also be present as well as α-Al_2O_3 in the region of special white high alumina cements. Upon the addition of water, CA and CA_2 hydrate to form intermediate reaction products with the final predominant stable phase being C_3AH_6.

Through the traditional use of calcium aluminate cement as a structural material, it was found that they possess several advantageous properties such as rapid strength development, chemical resistance, the ability to densify without shrinkage through the use of suitable systems, and the ability to form a refractory bond. However, a major disadvantage of calcium aluminate

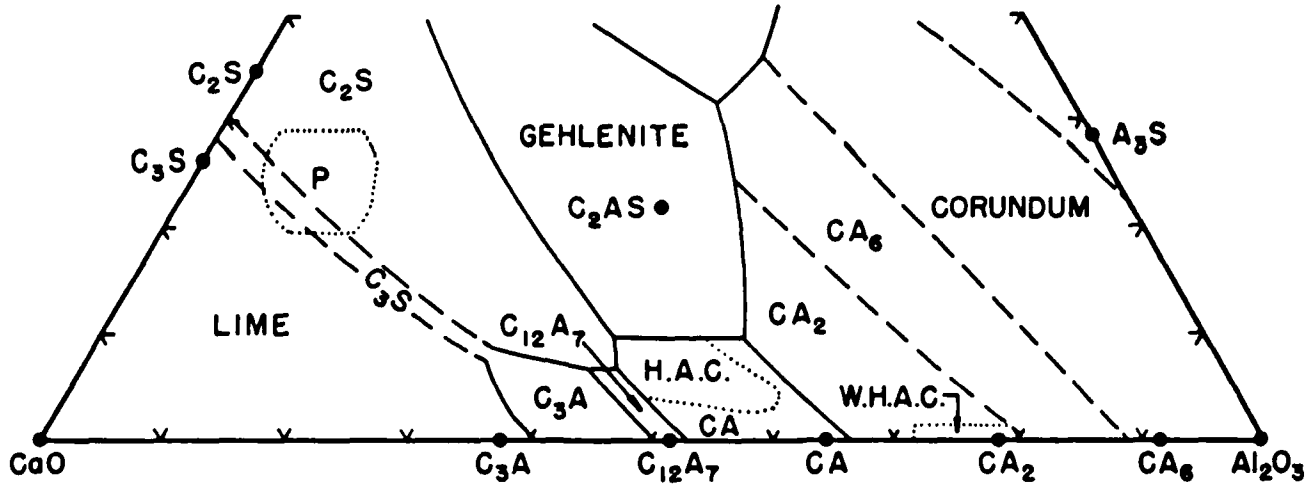

Figure 1. The Lime-Alumina-Silica System [1].

cements, as in all cements, is their inherent porosity. Bulk mechanical properties can be related to porosity and thus it is a key factor in controlling the ultimate strength of a cement. One approach to increasing the mechanical strength of a cement is based on eliminating all but the finest porosity (>10μ) to produce a macro-defect free (MDF) cement. The recent work of Birchall and co-workers indicates that cement produced by MDF processing has superior mechanical properties over conventionally processed cement [2-4]. Larger pores can be eliminated by reducing the water:cement (w/c) ratio ($\leq$0.20) and through the use of conventional ceramic processing (shear mixing, extrusion, die pressing, calendering). In addition, rheological control can be achieved by using water reducing agents, which act to control the charge on the surface double layer. Although the processing of any cement by the MDF method for use in industrial or commercial applications is relatively new, the ability of MDF cement to serve as an alternative to ceramic or even metals has already been demonstrated [5]. MDF cements have the ability to bond to metals and ceramics and therefore can be used as liners or in multilayer applications.

The concept of processing by the MDF method can be applied to calcium aluminate cements. The objective of this investigation is to process several grades of commercial calcium aluminate cement by the MDF method and to evaluate their dielectric properties for substrate applications.

Characterization of Precursor Cements

Eight types of commercial calcium aluminate cements supplied by Lone Star Lafarge, Inc. (Norfolk, VA) and Aluminum Company of America (ALCOA - Pittsburgh, PA) are reported. Initial characterization of these cements as-received includes: i) chemical composition, ii) phase composition, iii) density, iv) surface area and v) particle size distribution.

i) Chemical Composition

Table I summarizes the chemical composition of the cements as weight percent oxide content. The five Lone Star cements are classified as SECAR™ cement followed by a number depicting the weight percent Al_2O_3 content. ALCOA cements (type CA-25) are classified by application and possess similar chemistry. All of the calcium aluminate cements may be considered white high alumina cements comprised predominantly of Al_2O_3 and CaO, except SECAR 60, a high alumina cement containing a large quantity of SiO_2. Loss on ignition (LOI) includes CO_2 losses.

ii) Phase Composition

Phase composition by powder x-ray diffraction indicates a similarity in the phase composition of all of the calcium aluminate cements. Table II summarizes the phase composition of each of the cements. CA and CA_2 are the predominant phases with S, α-A, $C_{12}A_{14}$ present in varying amounts depending on the subtle variations in chemistry between cements. The presence of SiO_2 in SECAR 60 is expected since SECAR 60 is the only cement with a high enough Si chemical content to form a detectable Si compound.

iii) Density

Densities were obtained by pycnometry using a non-wetting liquid (kerosene) and measuring the volume displacement for a known weight of cement. Densities of the calcium aluminate cements range from 2.95 g/cc for SECAR 60 to 3.22 g/cc for ALCOA regular grade (Table II).

iv) Surface Area

Surface areas were obtained using gas adsorption on a known quantity of sample and range from 0.80 m^2/g for SECAR 71 to 12.64 m^2/g for ALCOA gunning grade. Surface areas are given in Table II.

Table I. Chemical Analysis of SECAR and ALCOA Calcium Aluminate Cements Expressed in Weight Percent Oxide.

	SECAR 60	SECAR 71	SECAR 80	SECAR 80 Fast Set	SECAR 80 Modified	ALCOA Gunning Grade	ALCOA Casting Grade	ALCOA Regular Grade
SiO_2	23.02%	0.52%	0.31%	0.32%	0.35%	0.30%	0.30%	0.32%
Al_2O_3	59.1	71.2	79.8	80.2	80.4	80.3	80.6	80.6
TiO_2	0.58	0.013	0.008	0.008	0.008	<0.05	<0.05	<0.05
Fe_2O_3	0.38	0.11	0.07	0.07	0.07	0.27	0.27	0.26
MgO	0.19	0.38	0.20	0.19	0.26	0.09	0.09	0.05
CaO	13.3	27.5	16.7	17.7	16.5	17.7	17.1	17.3
MnO	<0.002	<0.002	<0.002	<0.002	<0.002	0.060	0.062	0.064
SrO	0.01	0.01	0.01	0.01	0.01	0.005	0.005	0.005
Na_2O	0.22	0.37	0.74	0.45	0.95	0.51	0.58	0.56
K_2O	0.10	0.04	0.02	0.02	0.02	0.04	0.04	0.02
P_2O_5	0.05	0.02	0.13	0.02	0.01	0.11	0.12	0.10
SO_3	0.05	0.05	0.02	0.02	0.03	0.05	0.05	0.05
CO_2	(0.28)	(0.09)	(0.44)	(0.29)	(0.55)	0.06	0.07	0.06
LOI (900°)	3.60	0.36	1.55	0.80	1.54	0.77	0.93	0.80
TOTALS	100.60%	100.57%	99.56%	99.81%	100.15%	100.20%	100.15%	100.13%

Table II. Phase Composition, Density and Surface Areas of As-Received Calcium Aluminate Cements

Cement	Phase Composition*	Density (g/cc)	Surface Area (m^2/g)
SECAR 60	CA, CA_2, S	2.95	3.33
SECAR 71	CA, CA_2	2.96	0.80
SECAR 80	CA, CA_2, A	3.12	5.17
SECAR 80 Modified	CA, CA_2, A	3.15	6.24
SECAR 80 Fast Set	CA, CA_2, A	3.18	3.86
ALCOA Regular Grade	CA, CA_2, A, $C_{12}A_7$	3.22	8.10
ALCOA Gunning Grade	CA, CA_2, A, $C_{12}A_7$	3.16	12.64
ALCOA Casting Grade	CA, CA_2, A, $C_{12}A_7$	3.21	6.76

*Standard abbreviations in common use: S = SiO_2, A = Al_2O_3, C = CaO, H = H_2O.

v) **Particle Size Distribution**

Part size distribution of the cements by x-ray beam attenuation resulted in very similar curves. Typical mean particle size (50% cumulative mass percent) of the cements ranges from 2 to 10 micron.

Experimental Procedure

Samples were prepared for dielectric measurement by using a shear mixing process that involves the formation of a plastic cement dough by combining deionized water, calcium aluminate cement powder and 80% hydrolyzed polyvinyl alcohol (PVA). A typical mix consists of 11.11g of 10 wt% PVA solution and 50.00g of cement resulting in a w/c of 0.20 and a PVA/(water and cement) of 0.018.

The dough is first mixed by hand until all free PVA solution is absorbed then it is homogenized and trapped air removed by high shear mixing under vacuum in a C.W. Brabender preparation mill. The charge is typically 80cc in a batch. The resulting dough is then weighed into 2 to 3g charges placed in a 2.54 cm diameter steel die coated with a teflon mold release. Pressing into disks is accomplished by application of 138 MPa pressure for 10-15 seconds, followed by a slow release. The pressure cycle is repeated three times to ensure the escape of any trapped air in the sample. Each cement disk is removed from the die and placed into a dessicator over drierite at room temperature for curing.

Cement disks were prepared for permittivity measurement by sputter-coating gold electrodes onto either side of the disk followed by a spot of silver paint in each center for probe contact. Measurements were taken under ambient conditions on a computer controlled Hewlett-Packard multi-frequency LCR meter (Models 4274-A, 4275-A) that allows relative dielectric permittivity and dissipation factor (loss tangent) to be recorded as a function of

frequency from 100 Hz to 1 MHz. Several samples of each type cement were measured to ensure reproducibility.

Results and Discussion

Sample disks were on average (minimum of 5 samples) 2.51 mm thick and within 92% of theoretical bulk density.

Typical low frequency dielectric response for the calcium aluminate cements is given in Figure 2. The permittivities are quite low considering that the samples contain both unbound water and PVA. All of the ALCOA cements exhibit a similar response over the frequency range. However, the SECAR cements show a wide range of permittivities. Permittivities for the SECAR 80 series cements are enhanced by their α-Al_2O_3 content. In the SECAR 80 cements, during the fusion process to form slag, α-Al_2O_3 results from the deficiency of calcium necessary to combine with all of the aluminum in forming the cementitious calcium aluminate phases.

Conversely, SECAR 60 exhibits a remarkably low dielectric permittivity even though it contains a high percentage of potentially deleterious elements (Fe, Ti, Mg, Na). SECAR 60 is not considered to be one of the ultra-pure white high alumina cements and therefore has a much different chemistry. The high Si content allows for the formation of free SiO_2 (ε'~4) which effectively lowers the permittivity. SECAR 71 as seen from Figure 2, has a dielectric constant of ~5 and a flat frequency dependence due to the absence of α-A.

Dielectric loss in both SECAR and ALCOA cement samples is typically of the form shown for ALCOA casting grade in Figure 3, decreasing to ~2% at 1 MHz. In these cements cured under ambient conditions, the dominant transport of charge is the unbound water-PVA network, which is probably responsible for the large frequency dependence of dielectric permittivity and dissipation factor up to 10 kHz.

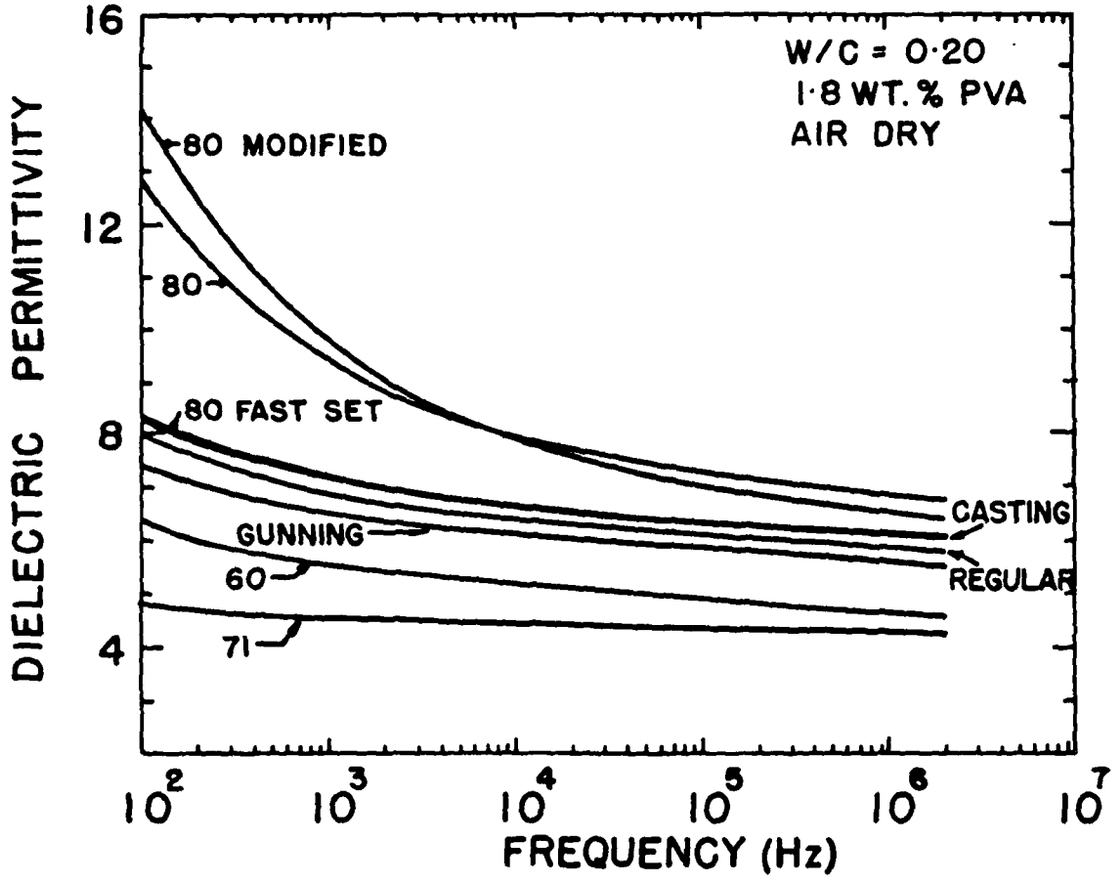

Figure 2. Relative dielectric permittivity of calcium aluminate cements containing 1.8 wt% PVA, a water-cement ratio of 0.20, cured in air as a function of frequency.

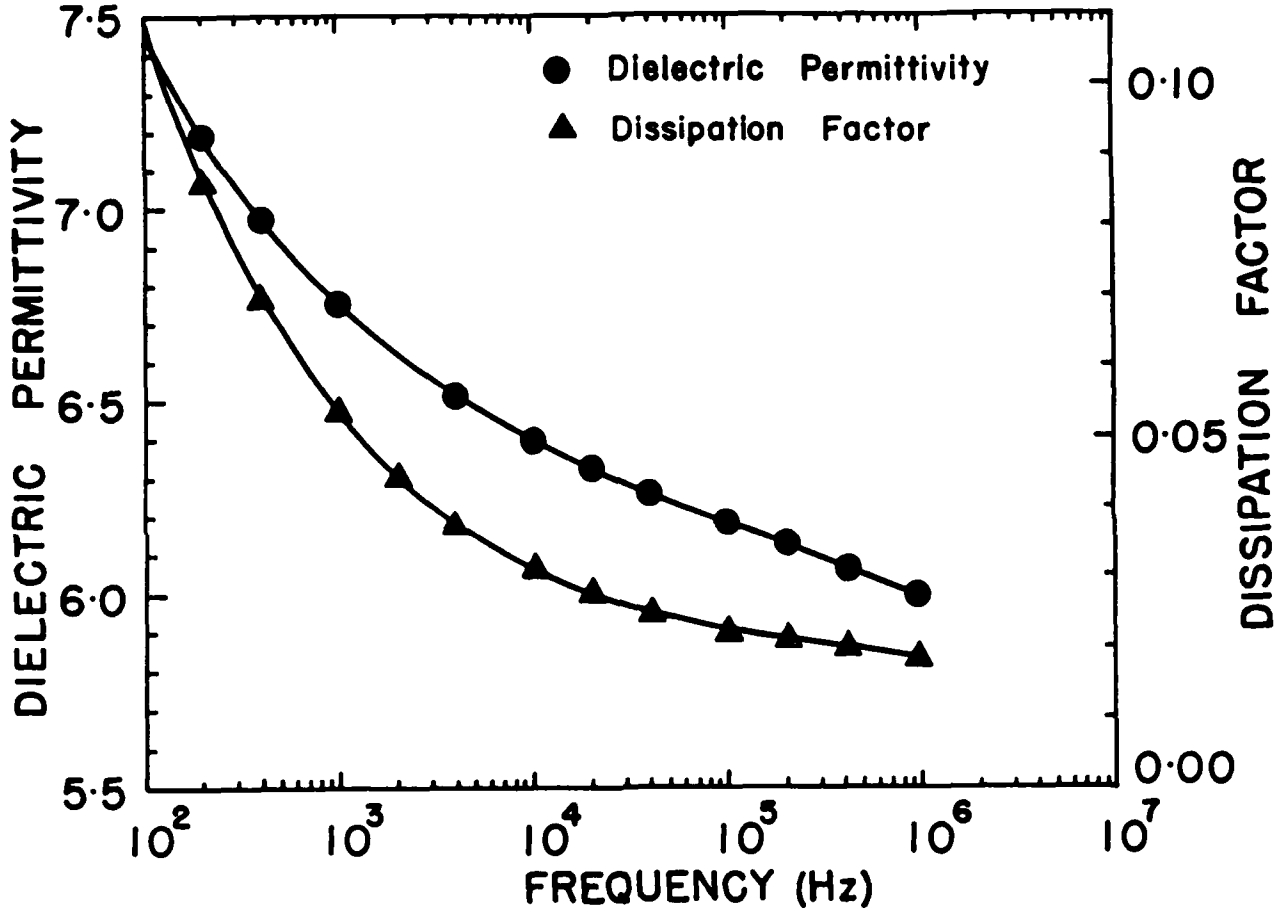

Figure 3. Relative dielectric permittivity and dissipation factor of ALCOA casting grade calcium aluminate cement containing 1.8 wt% PVA, a water-cement ratio of 0.20, cured in air as a function of frequency.

Summary

Among the eight different types of commercially available calcium aluminate cements investigated, SECAR 71 and 60 have the lowest dielectric permittivity (5 to 7) and dissipation factor of <0.02 at 1 MHz. The low frequency response of SECAR 60 and 71, along with the inherent advantages of calcium aluminate cement makes these cements good candidate materials for IC packaging applications.

Acknowledgement

The authors would like to thank both Lone Star Lafarge, Inc. and Aluminum Company of America for supplying the various cements. A special thanks goes to A. Kumar for drafting and Sharon Jows for typing. The work was supported by the Defense Advanced Research Projects Agency (ONR Contract N00014-84-K-0721).

References

[1] T.D. Robson, High-Alumina Cements and Concretes (Wiley and Sons, New York, 1962) p. 34.

[2] J.D. Birchall, A.J. Howard and K. Kendall, Nature 289 (1981) 388.

[3] J.D. Birchall, K. Kendall and A.J. Howard, V.S. Patent 4,353,748, October 12, 1982.

[4] J.D. Birchall, in: Proceedings of a Royal Society Discussion Meeting on Technology in the 1990's: Developments in Hydraulic Cements, ed. P. Hirsch (University Press, Cambridge, 1983) p. 31.

[5] N. McN. Alford and J.D. Birchall, in: Very High Strength Cement-Based Materials, Vol. 42, ed. J. Francis Young (Materials Research Society, Pittsburgh, 1985) p. 265.

APPENDIX IV

Accepted for publication in Materials Letters.

RELATIVE DIELECTRIC PERMITTIVITY OF CALCIUM ALUMINATE CEMENT-GLASS MICROSPHERE COMPOSITES

PAUL SLIVA, L.E. CROSS, T.R. GURURAJA AND B.E. SCHEETZ
Materials Research Laboratory, The Pennsylvania State University,
University Park, PA 16802, USA

Abstract

Calcium aluminate cement (SECAR^{TM} 80) was loaded with 0, 27.5, 40, 50, 60 and 70 volume percent hollow glass microspheres and processed macro-defect free by high shear mixing with polyvinyl alcohol as a rheological aid. Discs were formed by die-pressing and dielectric measurements obtained from 100 Hz to 2 MHz. Relative dielectric permittivity was lowered for all microsphere loadings and was lowest at 40 volume percent, corresponding to an effective porosity of 21.7 percent. A direct correlation was found to exist between microsphere loading (effective porosity) and the relative dielectric permittivity. Volume loadings of 27.5 and 40 percent microspheres resulted in the largest number of unbroken microspheres after processing. When compared with four ideal dielectric mixing models, the cement-microsphere composites were found to correlate best with Maxwell and Lichtenecker mixing.

Dissipation factor was lower over the measured frequency range for all microsphere loadings. No correlation was found to exist between effective porosity and dissipation factor. Dielectric losses at low frequencies can be attributed to unbound water and polyvinyl alcohol.

Introduction

Very large scale integration (VLSI) of GaAs integrated circuits has provided the impetus to develop new dielectrics for high density multilayer signal plane circuitry. Evolving packaging concepts have placed even more rigorous requirements on the selection of new materials. One of the most significant materials parameters necessary for dielectric substrates to be

used in signal plane applications is reduction of the dielectric permittivity to values less than 3.5. Present materials have relative dielectric permittivities in the approximate range of 5 to 10 including steatite (~6-8), cordierite (~5.8) and the most commonly used dielectric substrate, alumina (~9.8) [1].

In a previous paper, an evaluation of the dielectric response of several commercial calcium aluminate cements prepared by macro-defect free (MDF) processing, it was shown that pastes made from cements such as SECAR^{TM} 60, 71 and 80 (Lone Star Lafarge, Inc.) exhibit dielectric permittivities in the range of 4-14 at frequencies of 100 Hz to 1 MHz [2]. In addition, the dielectric loss of these cured cement pastes, although still containing polyvinyl alcohol and free water, is as low as 0.02 at 1 MHz. However, similar to other inorganic materials proposed or presently in use as dielectric substrates, MDF-processed calcium aluminate cement cannot attain the ultra-low relative permittivity required for packaging high speed GaAs integrated circuits. Therefore, an alternative approach to lowering the dielectric permittivity is to form a composite two-phase material using closed porosity as the second phase. A closed pore structure can reduce the dielectric permittivity of a material if it can be controlled to minimize dielectric losses.

This investigation is concerned with the feasibility of lowering the dielectric permittivity of calcium aluminate cement through the introduction of closed porosity via hollow glass microspheres. The glass microspheres are perceived to be chemically bonded into the densified cement matrix to form a discrete closed pore structure. Calcium aluminate cement with the addition of microspheres, processed MDF by conventional ceramic methods, would then result in a relatively high strength cured cement paste with minimal open porosity but an intimate distribution of closed porosity. Consequently, an additional

aspect of this study is to ascertain the volume fraction of closed porosity in the cured cement composites and to describe the distribution of the cement and microspheres by comparing the cured composites with one of several dielectric "mixing" models.

Experimental

In a previous study of eight different calcium aluminate cements produced commercially by both Aluminum Company of America (ALCOA Type CA-25: casting, gunning and regular grades) and Lone Star Lafarge, Inc. (SECAR 60, 71, 80, 80 fast set and 80 modified), it was shown that these cements exhibit dielectric permittivities from 4 to 14 between 100 Hz and 1 MHz [2]. Although samples prepared using SECAR 60 and 71 possessed the flatest frequency response of dielectric permittivity (between 4 and 6) and therefore have the highest potential for use as a dielectric substrate, SECAR 80 was chosen for this study. Secar 80 exhibits the highest dielectric permittivity of all the cements, ranging from ~13 at 100 Hz to ~7 at 1 MHz. Consequently, it is anticipated that subtle differences in the dielectric permittivity upon the addition of glass microspheres may be more pronounced in SECAR 80 as compared with SECAR 60 or 71.

i) Cement Characterization

Several physical properties of SECAR 80 calcium aluminate cement are given in Table I [2]. The predominant cementitious phase is $CaAl_2O_4$ with α-Al_2O_3 considered inert during hydration.

ii) Glass Microsphere Characterization

High strength hydrospace microballoon spheres are manufactured under the trade name Eccospheres FTD-202 by Emerson and Cuming (Dewey and Almy Chemical Division, W.R. Grace and Co., Canton, MA). Physical properties of the microspheres are given in Table I [3]. For compressive strength, given as

Table I. Physical Properties of SECAR 80 Calcium Aluminate Cement and Glass Microspheres.

SECAR 80

Chemical Composition (wt% oxide): 79.8% Al_2O_3, 16.7% CaO, 0.74% Na_2O, 0.31% SiO_2, 0.20% MgO, 0.25% (P_2O_5, Fe_2O_3, K_2O, SO_3, SrO, TiO_2, MnO), Loss on Ignition 1.55%

Phase Composition: $CaAl_2O_4$, $CaAl_4O_7$, α-Al_2O_3

Stable Hydrated Phase: $Ca_3[Al(OH)_6]_2$

Density: 3.12 g/cc

Surface Area: 5.17 m^2/g

Mean Particle Size (50% cumulative mass percent): 6 micron

Glass Microspheres

Chemical Composition (wt% oxide): 91.4% SiO_2, 2.22% B_2O_3, 1.36% Na_2O, 0.43% K_2O, 0.24% CaO, 0.16% Al_2O_3, 0.12% Fe_2O_3, 0.11% (P_2O_5, TiO_2, MnO, MgO), Loss on Ignition 4.84%

Average Particle Diameter (by weight): 65 micron

Average Wall Thickness (by weight): 1.2 micron

True Density: 0.238 g/cc

Bulk Density: 0.155 g/cc

Melting Temperature: 1100°C

Dielectric Constant (1 MHz to 8.6 GHz): 1.17

Dissipation Factor (1 MHz to 8.6 GHz): 0.0013

Volume Percent Survivors at 10.3 MPa Gas Pressure: 79.4

volume percent survivors, Emerson and Cumings suggests that there is a higher percentage of survivors when pressurized hydrostatically.

iii) Procedure

Samples were prepared for dielectric measurement by mixing together cement with a 10 wt% PVA solution and microspheres at loadings of 0, 27.5, 40, 50, 60 and 70 volume percent. Sample batches are given in Table II along with the water-cement ratio, wt% PVA and wt% microspheres for each.

The cement batches were prepared by first hand mixing until all of the PVA solution is absorbed and then shear mixing under vacuum in a preparation mill (C.W. Brabender Instruments, Inc., S. Hackensack, NJ) capable of 80.0 cc batches. The cement "dough" was removed after five minutes of mixing, weighed into 2-3 charges, and placed in a 2.54 cm diameter steel die. A teflon mold release was used to coat the die for easy sample removal. Discs were obtained by applying 6.2 MPa pressure followed by a slow release. The pressure cycle was repeated three times to allow for the escape of entrapped air in the cement paste. Each cement disk is removed from the die and placed into a dessicator over drierite at room temperature for curing.

For dielectric permittivity measurements, gold electrodes were sputter-coated onto both sides of the disk. A dot of silver paint was also placed into the center of either side for probe contact. Measurements were taken under ambient conditions on a computer controlled Hewlett-Packard mutli-frequency LCR meter (models 4274A, 4275A) that records the relative dielectric permittivity and dissipation factor (loss tangent) as a function of frequency from 100 Hz to 2 MHz. To ensure reproducibility, five samples of each batch were measured.

Results and Discussion

Relative dielectric permittivity as a function of frequency for cured SECAR 80/PVA cement paste plus loadings of 27.5, 40, 50, 60 and 70 volume

Table II. Contents of Cement Pastes Prepared with 0 to 70 Volume Percent Glass Microspheres.

Volume % Microspheres	Batch			Water/Cement	Weight% PVA	Weight% Microspheres
	SECAR 80 (g)	10 wt.% PVA Solution (g)	Microspheres (g)			
0	50.00	11.11	--	0.20	1.82[a] (1.82)[b]	--
27.5	50.00	11.11	2.45	0.20	1.82 (1.75)	3.85
40	50.00	11.11	4.20	0.20	1.82 (1.70)	6.43
50	50.00	11.11	6.53	0.20	1.82 (1.64)	9.65
60	50.00	11.11	9.69	0.20	1.82 (1.56)	13.81
70	50.00	11.11	15.10	0.20	1.82 (1.46)	19.81

a) with respect to (water + cement + PVA).
b) with respect to all solids.

percent glass microspheres is shown in Figure 1. The relative dielectric permittivity of the samples containing glass microspheres is lowered over the measured frequency range to some degree with the minimum occurring at 40 volume percent.

A fundamental consideration of the loading of glass microspheres into MDF-processed cement is the percentage of microsphere "survivors" after processing. In order to understand the dielectric response of a glass microsphere-cement composite, it is essential to be able to determine the volume fraction of closed porosity in the cured cement, or its "effective porosity."

The theoretical density for any cement-microsphere composite may be found by applying the linear relationship between theoretical density and volume percent microsphere loading in the following manner:

$$y = m(V_1)+n(V_2) \quad (1)$$

where y = theoretical density of the composite

m = density of the microspheres

V_1 = volume fraction microspheres in the composite

n = theoretical density of the cement-PVA mix

V_2 = volume fraction cement-PVA mix in the composite.

Theoretical density of the cement-PVA mix, n in equation (1), can be established at zero percent microsphere loading which is the y intercept. The pure cement-PVA mix is comprised of 59 vol% SECAR 80 and 41 vol% PVA solution. Multiplying each volume fraction by its density, 3.12 g/cc and ~1 g/cc, respectively, and then adding, results in a theoretical density of 2.25 g/cc. Subsequent use of 2.25 g/cc as the baseline density for the cement-PVA mix enables the theoretical densities of microsphere-loaded samples to be determined from equation (1) and are given in Table III. As expected with the

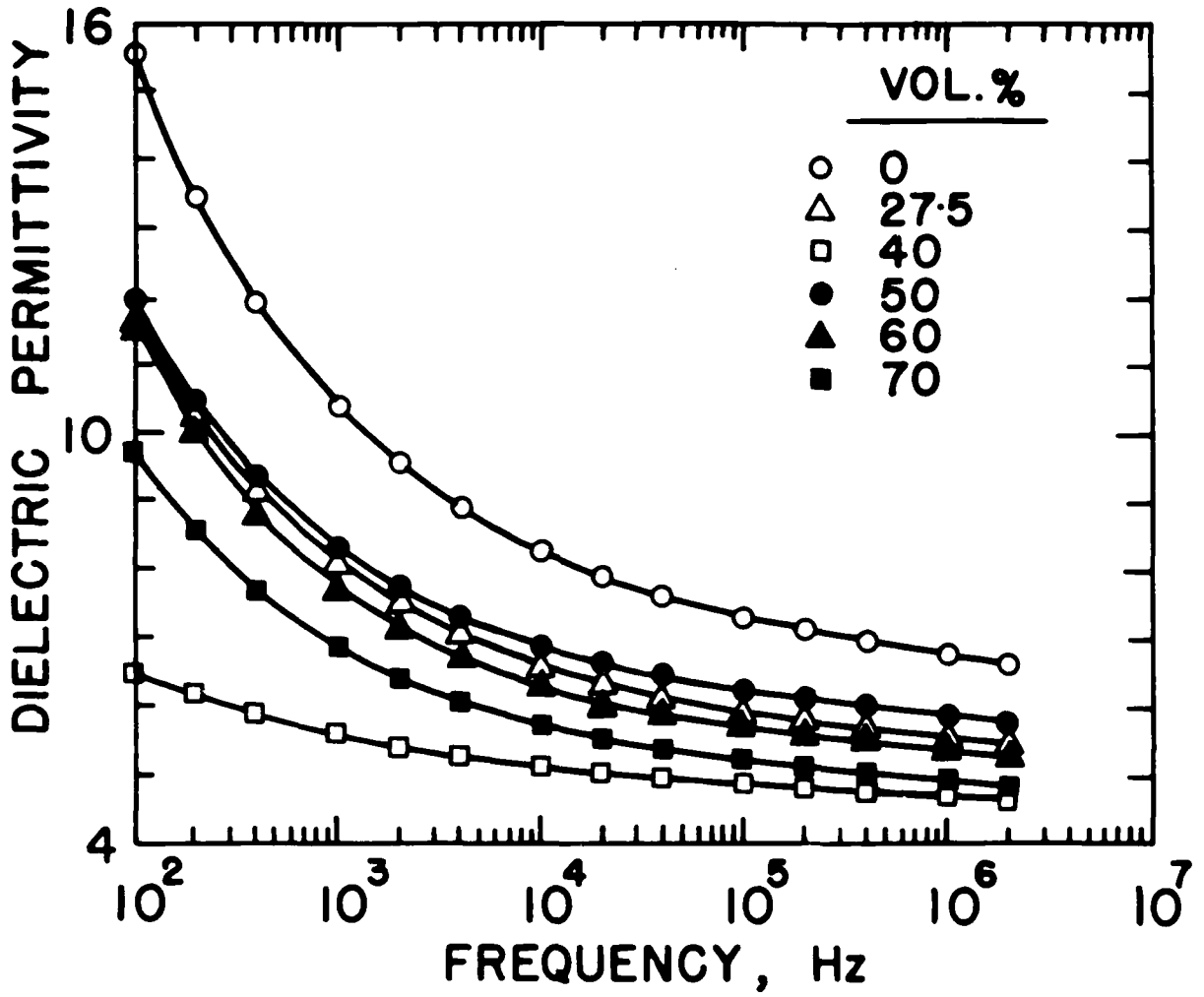

Figure 1. Relative Dielectric Permittivity as a Function of Frequency for Calcium Aluminate Cement (Secar 80) Containing 0 to 70 Volume Percent Glass Microspheres.

Table III. Theoretical and Geometric Densities, Percent Microsphere Survivors and Effective Porosity of Cements Prepared with 0 to 70 Volume Percent Glass Microspheres.

Volume Percent Microspheres	Theoretical Density (g/cc)	Geometrical Density (g/cc)	Percent Survivors	Effective Porosity
0	2.25	2.22	--	--
27.5	1.70	2.01	40%	10.6%
40	1.46	1.79	54	21.7
50	1.24	2.01	21	10.6
60	1.04	1.94	24	14.1
70	0.85	1.83	28	19.7

loading of a less dense phase, the slope of equation (1) is negative and the theoretical density decreases with increasing microsphere content.

Geometrical densities of the six different microsphere loadings are the average of five cured cement discs within each loading series and are listed in Table III. A comparison of the theoretical and measured densities for cured cement-PVA discs (no loading) shows that the cured cement is within 98% of theoretical. A comparison of the microsphere-loaded cement samples indicates that for a given microsphere loading, the resultant density is much higher than predicted. Consequently, it is possible that microspheres are breaking during processing and therefore reducing the effective porosity.

Determination of the effective porosity for each loading can be accomplished in the same manner as the theoretical densities by again applying the linear relationship depicted in equation (1). Conversely, the measured geometric densities may now be used to calculate the final volume percent microspheres in a sample as follows:

$$y = 0.238V_1 + 2.22(1-V_1) \qquad (2)$$

where y = measured density of the composite

V_1 = effective volume percent microspheres in the composite

$(1-V_1)$ = volume percent cement-PVA mix plus broken microspheres.

In equation (2), 0.238 is the density of the glass microspheres and 2.22 is the measured density of the cured cement with no microspheres which therefore may be considered a baseline matrix density. A major premise of equation (2) is that broken microspheres are approximately of the same density as the cured cement and therefore may be included in the $(1-V_1)$ term.

Effective porosity for each microsphere loading, expressed as a percentage of the total composite, is given in Table III. The difference between initial loading and effective porosity (final loading) is also given

in Table III as percentage of surviving microspheres. From comparing the measured densities of the cured samples to the effective porosity, it is apparent that a direct correlation exists.

A comparison of the effective porosity with the relative dielectric permittivity for each microsphere loading as a function of frequency shows a direct correspondence between the two (Figure 1). Microsphere loadings of 27.5, 50 and 60 volume percent give a similar dielectric response as expected from effective porosities of 10.6, 10.6 and 14.1%, respectively. The microsphere loading of 40 volume percent depressed the dielectric permittivity the greatest which is expected from the largest effective porosity of all the loaded samples (21.7%). An effective porosity of 19.7% for the initial 70 volume percent microsphere-cement composite predicts a dielectric response between the initial 40 and 60 volume percent microsphere cements which is evident from Figure 1.

The ability to predict the dielectric response of cement-microsphere composites from the effective porosity provides a direct correlation between microsphere loading and the resultant lowering of the relative dielectric permittivity. Additionally, systematic lowering of the dielectric permittivity over the total measured frequency range further indicates only a single contributing mechanism, the glass microspheres. Although breakage of glass microspheres is evident at all volume percent loadings, it is presumed that at loadings of greater than 40 volume percent, the cement is unable to screen the microspheres, resulting in an even greater amount of breakage. This effect is evident from the percent of microsphere survivors shown in Table III. Volume percent loadings of 27.5% and 40% resulted in 40% and 54% survivors in the final composite, respectively, with a dramatic drop in survivors for higher loadings.

Dielectric Mixing

A basic approach to determining the mixing of closed porosity into a dielectric matrix material is one of two phase interconnectivity which may be described by various types of dielectric mixing. Dielectric mixing rules are based on distinct microstructural arrangements, each providing an average dielectric permittivity for any composite using only the volume fraction and relative dielectric permittivity of each phase. The introduction of hollow glass microspheres into a cement matrix involves two phases, if the closed porosity that the microspheres provide is considered a second discrete phase. An average dielectric permittivity of any cement-microsphere composite may then be determined from 0 to 100% porosity (i.e. percent microsphere loading) using each of the mixing rules: series and parallel capacitive mixing, Lichtenecker's logarithmic (3-dimensional interconnectivity) and Maxwell's mixing model (spherical, homogeneously distributed pores in a continuous matrix).

The four mixing rules are presented in Table IV and are graphically represented in Figure 2 for cement-microsphere composites at 1 MHz. Relative dielectric permittivities of 6.8 and 1.17 taken at 1 MHz for the cement and glass microspheres, respectively, were used to determine the curves. The parallel and series mixing models represent end members and thus provide upper and lower bounds of relative dielectric permittivity. Maxwell's and Lichtenecker's models provide a compromise between the end members and depict a type of three-dimensional homogeneous connectivity of the phases.

As is evident from the cement-microsphere composite microstructure, the average dielectric permittivity will lie between the two bounding cases. Using the relative dielectric permittivity of each composite at 1 MHz and its known effective porosity, the five cement-microsphere composites are plotted on Figure 2 and as predicted, the microstructures are best described as a

Table IV. Dielectric Mixing Rules for Two Phase Composites [4].

$$\frac{1}{K} = \frac{V_1}{K_1} + \frac{V_2}{K_2}$$

a) Series Mixing

$$K = K_1V_1 + K_2V_2$$

b) Parallel Mixing

$$\ell nK = V_1 \ell nK_1 + V_2 \ell nK_2$$

c) Lichtenecker's Logarithmic Mixing

$$K = \frac{V_2K_2(\frac{2}{3} + \frac{K_1}{3K_2}) + V_1K_1}{V_2(\frac{2}{3} + \frac{K_1}{3K_2}) + V_1}$$

d) Maxwell's Mixing

K = average relative dielectric permittivity
K_1, V_1 = relative dielectric permittivity and volume fraction of phase one
K_2, V_2 = relative dielectric permittivity and volume fraction of phase two

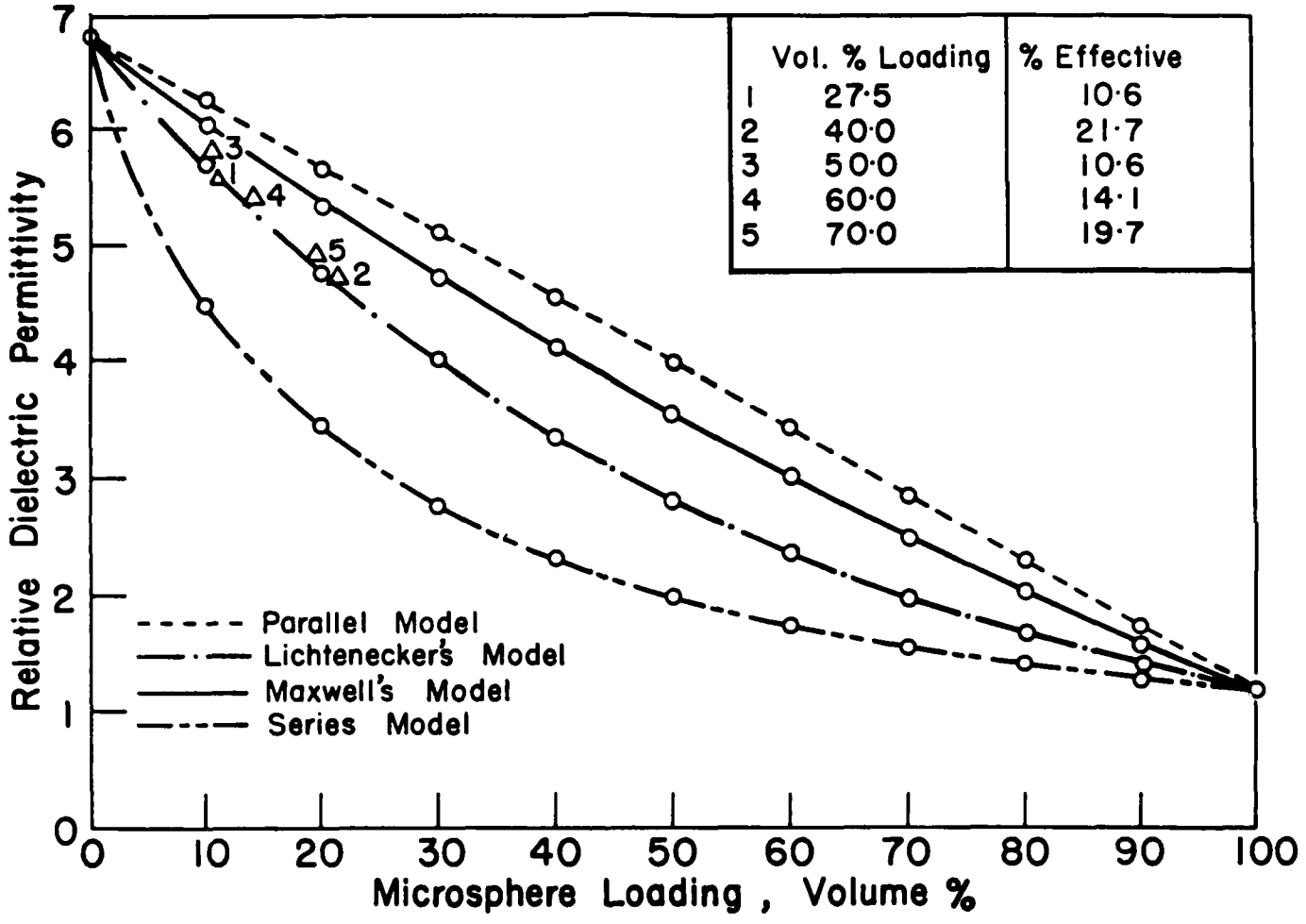

Figure 2. Relative Dielectric Permittivity of Cement-Microsphere Composites as a Function of Volume Percent Microsphere Loading for Series, Parallel, Maxwell's and Lichtenecker's Mixing Rules.

combination of mixing rules. Maxwell's as well as Lichtenecker's models provide the closest approaches to describing the composite microstructure.

Dissipation factor for the cement-PVA matrix and microsphere-loaded samples as a function of frequency is shown in Figure 3. All of the composite samples lowered the dissipation factor to some extent. There is a direct correlation between original volume percent microsphere loading and dissipation factor with the loss increasing with total volume percent microspheres. There does not appear to be any correlation of dissipation factor to effective porosity as effective porosities of 21.7% and 10.6% resulted in the same loss behavior. Losses at low frequencies are assumed to be due to the unbound water-PVA network still present in cement pastes cured under ambient conditions.

Summary

SECAR 80 cement-microsphere mixes resulted in a lower relative dielectric permittivity for all volume percent loadings over the frequency range of 100 Hz to 2 MHz. Although a considerable number of the microspheres were destroyed during processing, a direct correlation was found to exist between the densities of the cured composites, the final volume percent of microspheres or the effective porosity, and the dielectric permittivity. Application of this approach of introducing a closed pure structure into the cement could obviously be further enhanced by using a stronger microsphere or providing "softer" processing. Additionally, although SECAR 80 was used in this study for demonstration purposes, SECAR 60 or 71 would provide a much better baseline matrix material for further reduction of the dielectric permittivity [2]. For example, the relative dielectric permittivity of 4.3 for SECAR 71 (at 1 MHz) would require the addition of only 20 volume percent microspheres to lower the dielectric permittivity of the composite to 3.30 and

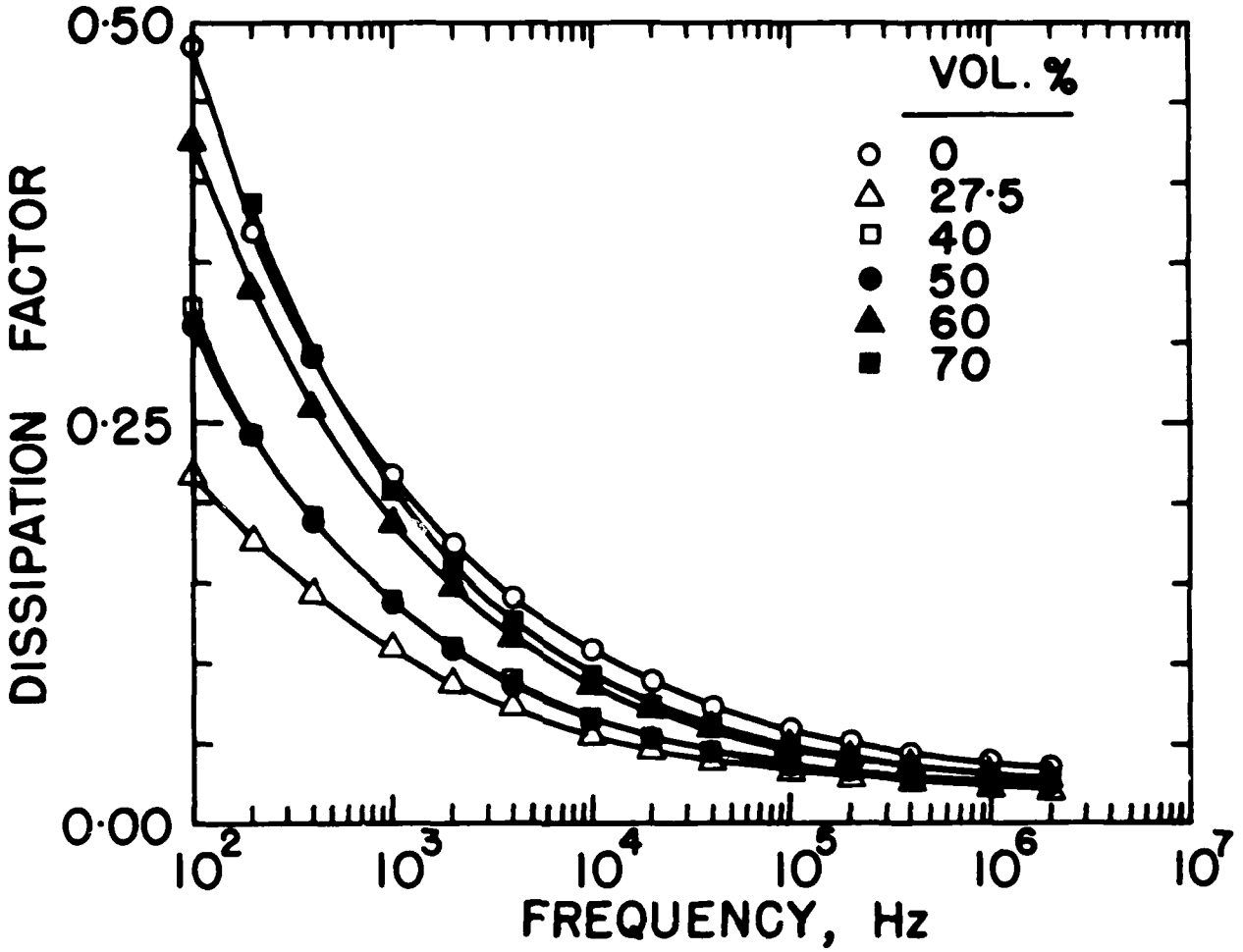

Figure 3. Dissipation Factor as a Function of Frequency for Calcium Aluminate Cement (Secar 80) Containing 0 to 70 Volume Percent Glass Microspheres.

30 volume percent microsphere to reduce the dielectric permittivity to 2.9. Microsphere loadings of this size (20-30 volume percent) would not only result in a higher strength material but as shown in this study for microsphere loadings of 40 volume percent of less, a higher survival rate of initial microspheres. The close correlation between the cured cement-microsphere composites and the Maxwell and Lichtenecker dielectric mixing models provides a simple approach to approximating other composites of similar nature. Although no correlation could be found between effective porosity and dissipation factor, the dissipation factor was lower for all of the cements containing microspheres. No particular loss mechanism other than the unbound water-PVA network contributing at low frequencies could be established.

Acknowledgement

The authors would like to thank Lone Star Lafarge, Inc. for supplying the SECAR 80 and Emerson and Cuming for the FTD-202 glass microspheres. A special thanks goes to A. Kumar for drafting and Sharon Jows for typing. This study was supported by the Defense Advanced Research Projects Agency (ONR Contract N00014-84-K-0721).

References

[1] Dielectric Materials and Applications, Edited by Arthur R. von Hippel (MIT Press, Cambridge, 1966) p. 301.

[2] P. Sliva, L.E. Cross, T.R. Gururaja and B.E. Scheetz, Mat. Letters (submitted).

[3] Emerson and Cuming Technical Bulletin, 14-2-4B, Revised 4/78.

[4] A.R. von Hippel, Dielectrics and Waves (Wiley and Sons, New York, 1954).